THE DECAY PHASE OF SOLAR FLARE EVENTS

K. G. McCRACKEN*, U. R. RAO**, R. P. BUKATA, and E. P. KEATH
The University of Texas at Dallas, Dallas, Texas, U.S.A.

(Received 21 October, 1970)

Abstract. A study of the properties of the cosmic radiation of energy $\simeq 10$ MeV generated by solar flares is reported. Data from four Pioneer spacecraft in interplanetary orbits, and separated by $\sim 180°$ in heliocentric longitude are employed. Attention is restricted to the properties evident at times in excess of 1 day after the occurrence of the parent flare. The anisotropic character of the radiation; the gradients in heliocentric longitude; the decay time constants; and the energy spectra of the radiation are all studied in detail.

It is found that the equilibrium anisotropy assumes a direction $\simeq 45°$ E of the satellite-Sun line at very late times. It is suggested that the anisotropy at such times is parallel to $\mathbf{E} \times \mathbf{B}$. This observation confirms that convection is the determining process in the escape of the solar cosmic rays from the solar system. It indicates that a positive radial gradient of solar cosmic radiation density has built up at orbit of Earth some 4 days after a flare. This results in an effective convective velocity of approximately $\frac{1}{2}$ the solar wind velocity. Direct measurements indicate the presence of strong gradients in heliocentric longitude even at very late times ($\gtrsim 4$ days). These gradients are essentially invariant with respect to time. e-folding angles of $\eta \simeq 30°$ have been observed at $\simeq 10$ MeV. The presence of these gradients has a major effect on the temporal variation of the cosmic ray flux during the decay phase of the flare effect. Thus, the observed decay time constant is either increased or decreased relative to the 'convective' value depending on the position of the observer relative to the centroid of the cosmic ray population injected by the flare. The effect of the gradient becomes more pronounced at lower energies, and may even exceed the convective removal rate. The observed decay time constant, the characteristics of the anisotropy, and the gradient in longitude are shown to be inter-related as demanded by theory. It is shown that the exponent of the cosmic ray spectrum is dependent on the location of the observer relative to the centroid of the cosmic ray population injected by the parent flare. At a given point in the frame of reference of the cosmic ray population, the spectral exponent is invariant with time.

1. Introduction

In the past several papers (e.g. McCracken *et al.*, 1967, 1968; McCracken and Rao, 1970) we have shown that the cosmic ray anisotropy during solar flares is large and field aligned initially which then changes to an equilibrium type of anisotropy during the decay phase of the flare effect. The equilibrium anisotropy was found to be always directed radially outward from the Sun. In this paper we show that the radially directed equilibrium anisotropy observed during the early part of the decay evolves finally into an equilibrium anisotropy from the East during late times in the decay. Besides the anisotropy characteristics, we present, in this paper, a detailed study of the decay phase of the solar flare effect, in particular, the spatial gradients, the temporal decay and the spectral properties of the radiation.

* Now at CSIRO, G.P.O. Box 124, Port Melbourne, Victoria 3207, Australia.
** On leave from Physical Research Laboratory, Ahmedabad, India.

Solar Physics **18** (1971) 100–132.

TABLE I

Physical characteristics of cosmic ray anisotropy detectors on board the Pioneers 6, 7, 8, and 9 spacecraft

Spacecraft	Launch date	Period days	Perihelion/Aphelion AU	Nominal energy windows (omnidirectional data)	Directional measurements	Data coverage during 1967 Nov.–1969 April
Pioneer 6	1965, Dec. 16	311.3	0.81–0.94	7.5–45/45–90 MeV	4	$\simeq 10\%$
Pioneer 7	1966, Aug. 17	402.9	1.01–1.13			
Pioneer 8	1967, Dec. 13	386.6	0.99–1.09	4.5–45 MeV in 6 energy bands	8	$\geqslant 50\%$
Pioneer 9	1968, Nov. 8	297.6	0.75–0.99		8	$\geqslant 75\%$

2. The Source of the Observations

The data reported herein were obtained by cosmic ray detectors on the four interplanetary spacecraft, Pioneers 6 through 9. The characteristics of these detectors are summarized in Table I.

For the purposes of this paper, we have restricted our attention to the period 8 November, 1968 to 30 April, 1969, since good coverage was obtained for all four spacecraft during this time (see Table I), and further, there were a number of well defined flare events. The positions of the spacecraft relative to the Earth during this interval are shown in Figure 1.

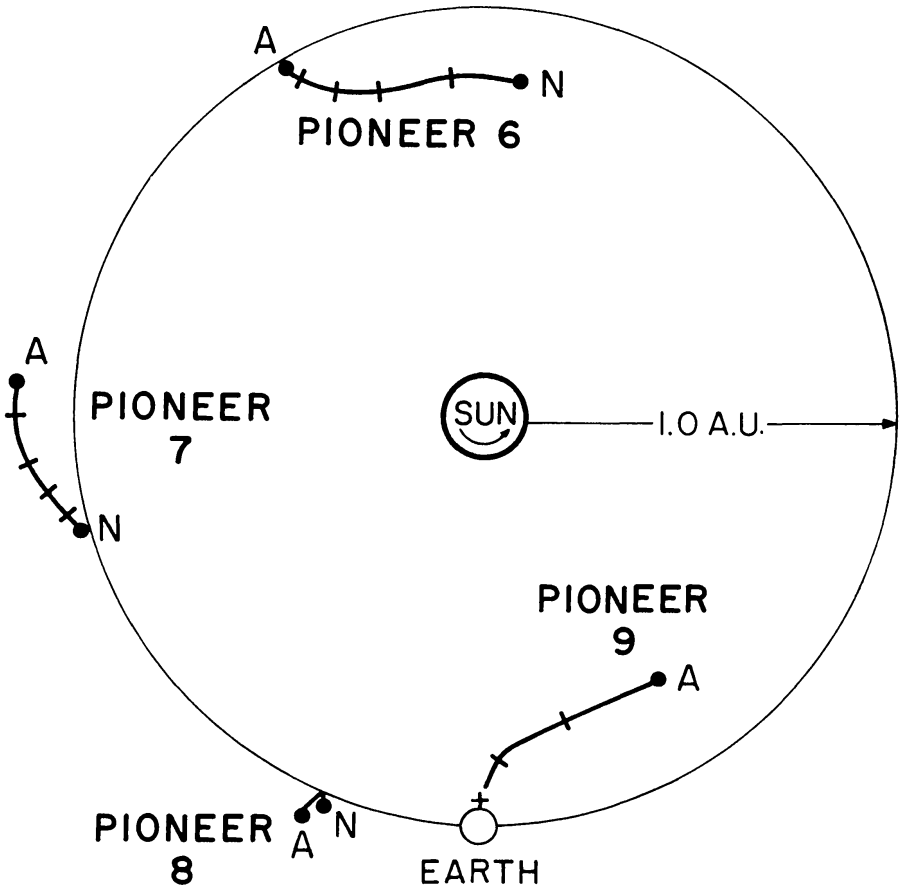

Fig. 1. The positions of the four Pioneer spacecraft during the period November 1968 (N) to April 1969 (A).

The instruments have been described elsewhere (Bartley *et al.*, 1966; Bukata *et al.*, 1970). The data handling procedures for Pioneers 6 and 7 have been outlined earlier (McCracken *et al.*, 1967), and those for Pioneers 8 and 9 are basically similar. Suffice to say that the latter spacecraft provide 8 directional fluxes (on 45° centers), and 6 energy spectral windows from detectors broadly similar to those on Pioneers 6 and 7. Pioneers 8 and 9 are also equipped with a solid state detector, however, the data from this instrument will not be considered herein.

Am^{241} radioactive sources incorporated into the detectors have permitted the detection of small changes in the energy calibrations of the instruments. The changes were insignificant for all instruments except that on Pioneer 8. The data from the latter spacecraft have been fully corrected for the changes that occurred.

All times reported herein have been corrected for the transit time of the telemetry signals. The characteristics of the data from the several detectors are such that there is absolutely no possibility of inadvertant interchange of the data of two spacecrafts.

3. The Equilibrium Anisotropy of the Decay Phase

Since it has an important bearing on the nature of the mechanism whereby the solar cosmic rays leave the solar system, we first discuss the cosmic ray anisotropy at late times in the decay phase of a flare effect.

We have previously shown that the cosmic ray anisotropy becomes aligned with the solar wind velocity vector some 12–24 hr after the injection of the cosmic rays into the solar system (McCracken *et al.*, 1967, 1968). This behaviour has been explained in terms of the cosmic ray 'current' having become predominantly due to convective removal of the cosmic rays by the moving solar wind (Parker, 1965; McCracken *et al.*, 1968; Forman, 1970). This implies dominance of the convective current over the diffusive component of the cosmic ray current, i.e. it implies

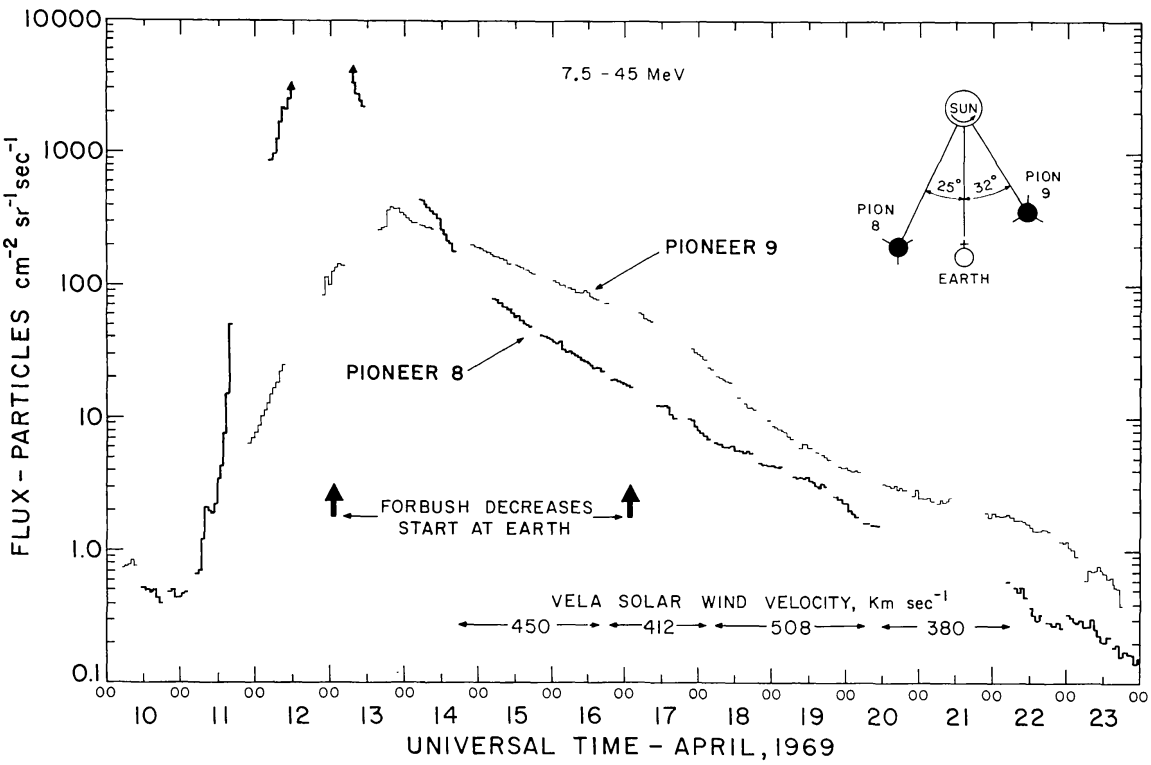

Fig. 2. The temporal variations of the 7.5–45 MeV cosmic ray fluxes observed by Pioneers 8 and 9 during the flare effect of 1969, April 11. The Pioneer 8 flux should be multiplied by a factor of 1.7. The Vela solar wind velocities have been shifted in time to indicate the solar wind variability at Pioneer 9.

$(2+\alpha\gamma)V_p \gg 3(K\cdot\nabla U)\,U^{-1}$, or that the gradient in U is small. Note that the following symbols will be used freely throughout this paper:

V_p = solar wind velocity
v = cosmic ray velocity
U = cosmic ray density
K = diffusion tensor
γ = the exponent in the power law fit to the cosmic ray spectrum

$$dJ(E) = \text{const. } E^{-\gamma}\,dE$$

and

$$\alpha = \frac{T_{cr} + 2m_0c^2}{T_{cr} + m_0c^2}$$

where T_{cr} is the kinetic energy of the individual cosmic rays.

In Figure 2 are displayed the data for a solar flare that occurred on April 11, 1969. It is clear that a simple, quasi-exponential decay of the intensity was evident over a region of space exceeding $\sim 50°$ in heliocentric longitude. We have therefore studied this event in some detail in order to provide an insight into the decay phase of the solar flare effect.

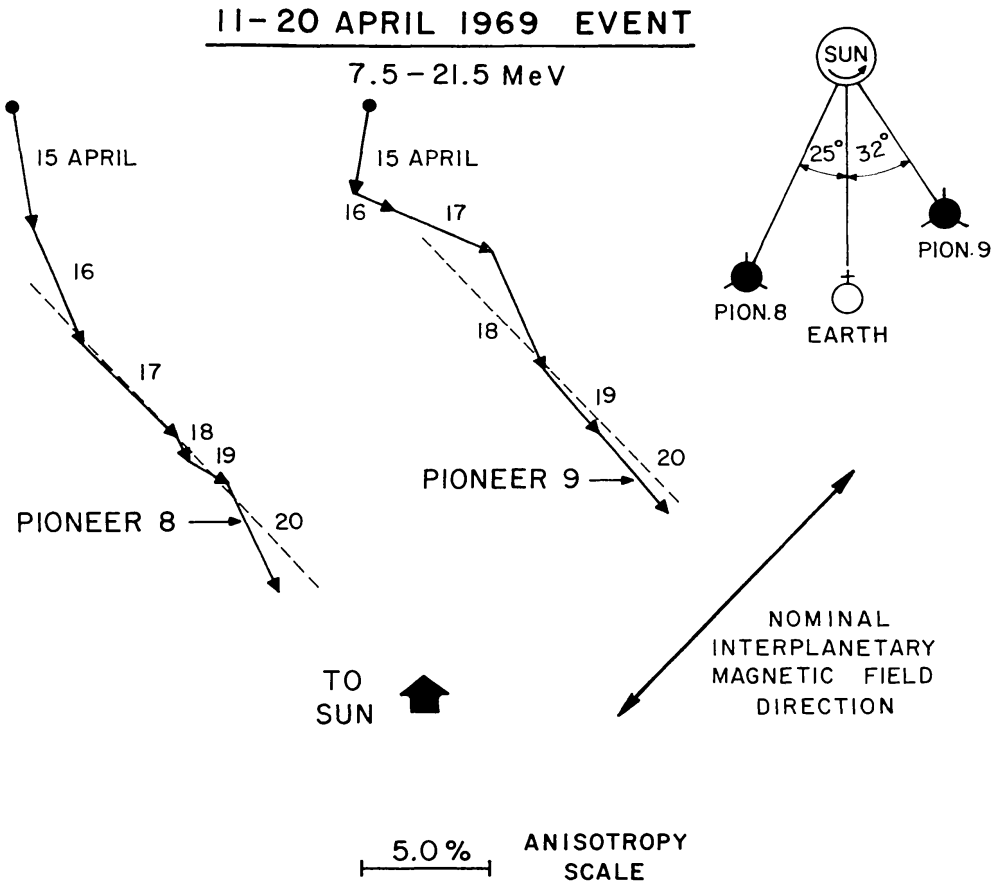

Fig. 3. The cosmic ray anisotropy vector diagrams for Pioneers 8 and 9 for the decay phase of the flare effect of 1969, April 11. The dashed line is drawn 45° to the East of the spacecraft-Sun direction.

Figure 3 displays the daily mean anisotropy of 7.5–21.5 MeV protons observed by Pioneers 8 and 9 during the latter part of the decay phase of this event. It is clear that while the anisotropy was initially directed radially away from the Sun, its vector direction was from the East of this direction at very late times. In this regard it will be noted that the behaviours were essentially identical at the two spacecraft. The long lived nature of the anisotropy from the East (for a total period of >4 days, i.e. 16–20 April 1969) indicates that it is most unlikely that this Easterly anisotropy was due to an anisotropic flow streaming along anomalous interplanetary lines of force (i.e., with the magnetic vector $\simeq 45°$ E of the Earth-Sun line, as contrasted with the normal value of $\simeq 45°$ W).

Anisotropies have been observed from the East of the satellite-Sun line at late times in other flare events. Thus both the ionic and electronic cosmic radiation exhibited such anisotropies during the decay of a long lived flux enhancement in November 1967 (Allum *et al.*, 1971; Rao *et al.*, 1971). Other evidence of a similar nature has also been found for other flare events in the data obtained by our laboratory's cosmic ray anisotropy detector on the Explorer 34 spacecraft. Furthermore, reference to Figure 18 of McCracken *et al.* (1967), shows that the anisotropy of the radiation during the decay phase of the event of 1966, September 26, had swung around to $\sim 35°$ E by 1966, October 1.

Figure 4 presents further anisotropy data for very late times in three large flare effects observed by both Pioneers 8 and 9. It is abundantly clear that, without exception, the anisotropy was from an easterly direction at late times ($T \gtrsim 4$ days). The reason that this was not noted previously is largely due to the fact that we have observed relatively few flares that were intense enough to permit definitive anisotropy measurements at such a late time in the decay phase.

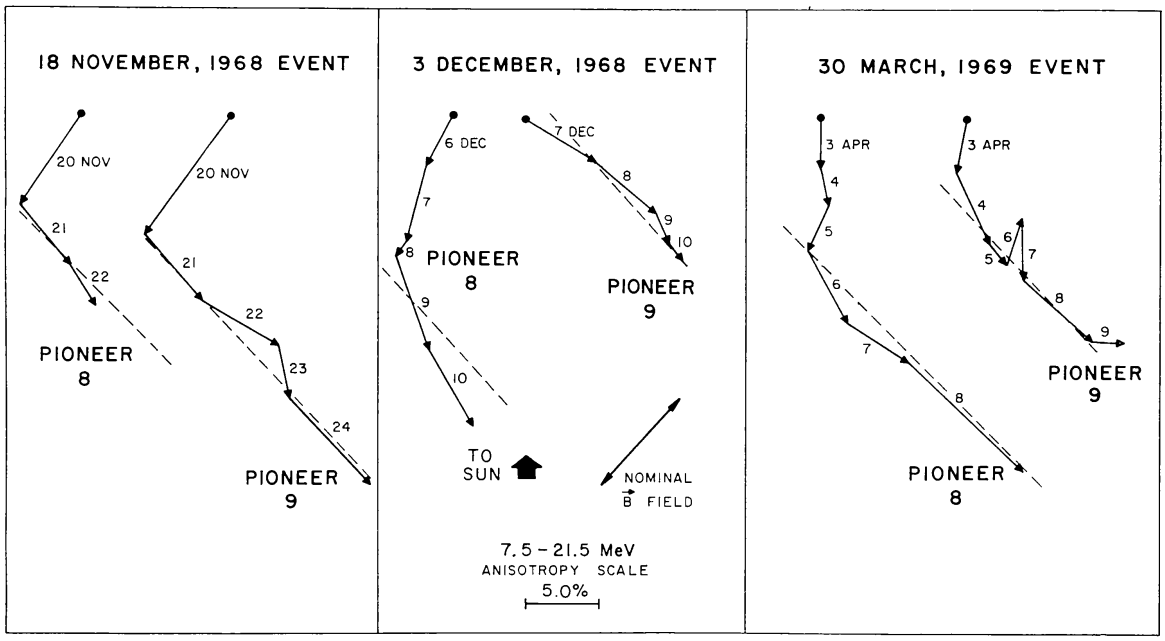

Fig. 4. The cosmic ray anisotropy vector diagrams for Pioneers 8 and 9 for the decay phases of three flare effects. The dashed lines are drawn 45° to the east of the spacecraft-Sun direction.

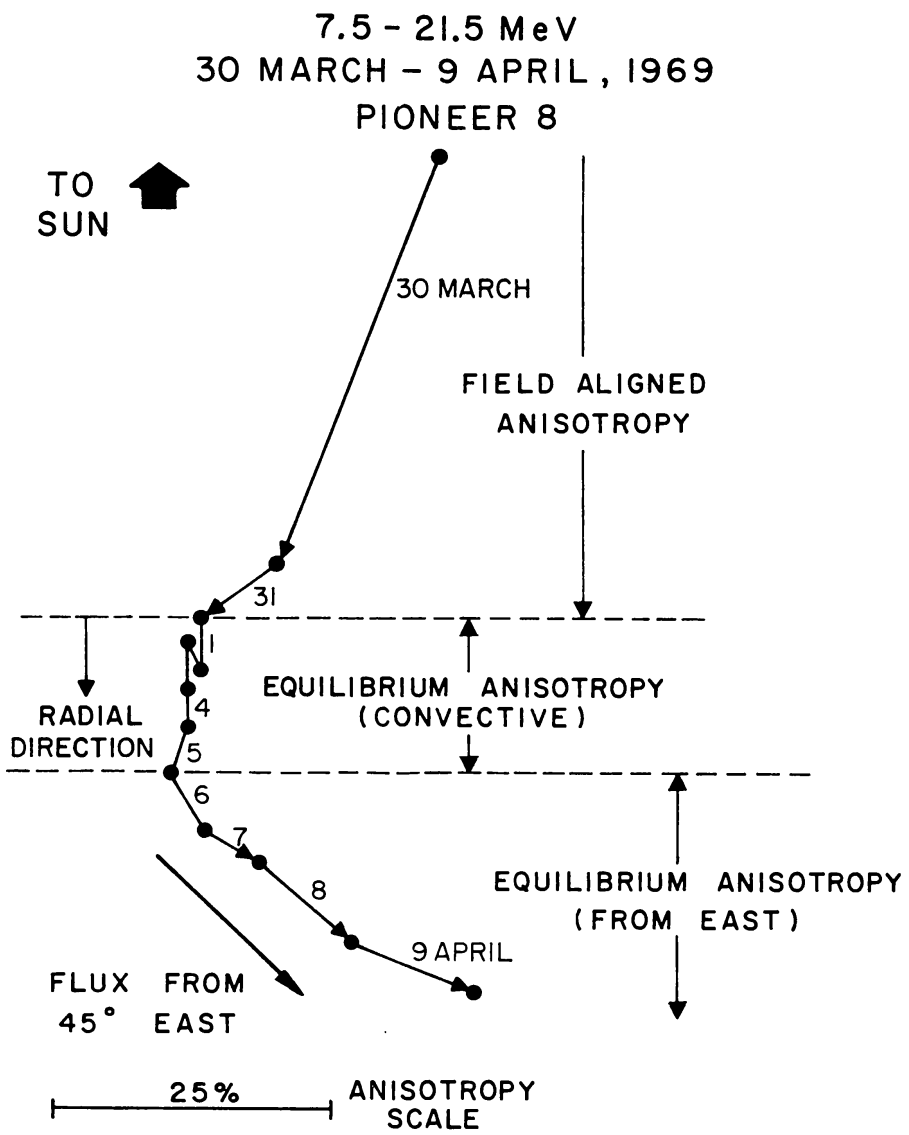

Fig. 5. Illustrating the evolution of the anisotropy of solar cosmic radiation. The parent flare occurred late on 1969, March 29. The vectors are the average anisotropy vectors for each calendar day thereafter.

Figures 5 and 6 summarize the evolution of the cosmic ray anisotropy during a solar flare effect. Both confirm the well known fact that the anisotropy is generally directed from the West at early times in the flare, and that it is of large amplitude. This type of anisotropy indicates a significant diffusive component $K\nabla \cdot U$ directed away from the Sun, and parallel to **B**, the interplanetary magnetic field vector. This model is illustrated in Figure 7. Figures 5 and 6 further show that an anisotropy then develops that is directed radially ($\pm 20°$) away from the Sun. The radially directed equilibrium anisotropy which was first noted in our Pioneer 6 data, has already been extensively discussed in the literature (McCracken *et al.*, 1967, 1968; Forman, 1970; McCracken and Rao, 1970). It is clear that radially directed anisotropy, indicative of purely convective removal of the cosmic radiation, occurs in the interval 1 to 4 days

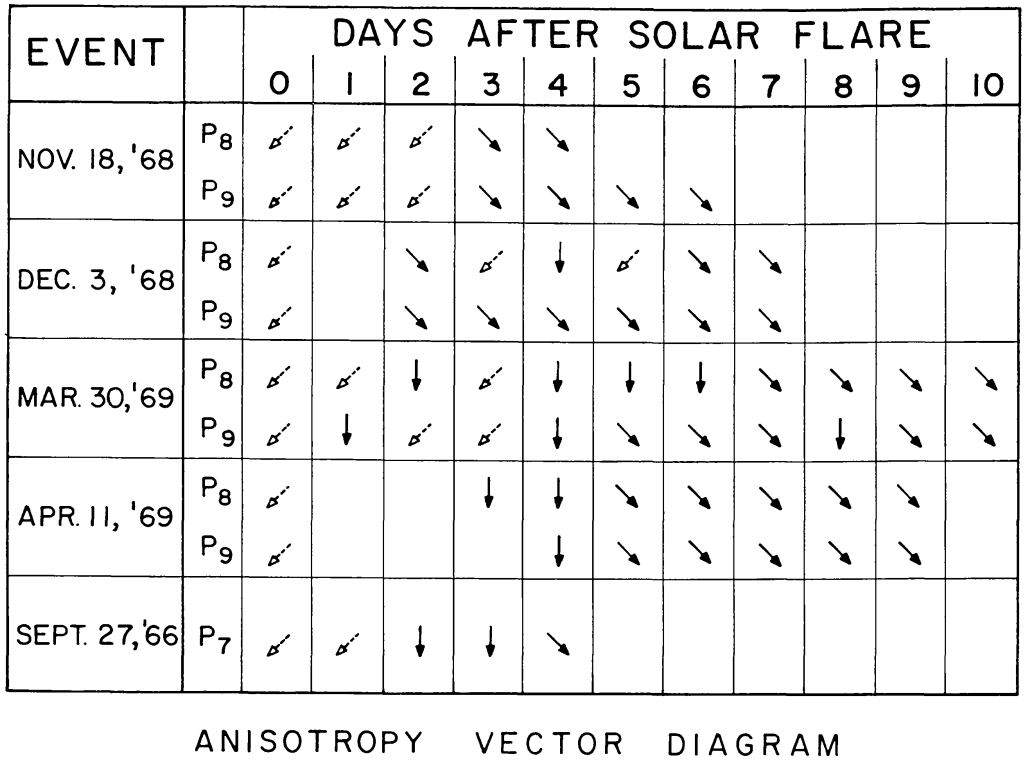

Fig. 6. Summarizing the vector directions of the cosmic ray anisotropy during 5 solar flare effects. A dotted arrow to the left indicates an anisotropy which was from the West of the spacecraft-Sun line; a solid arrow to the right indicates an anisotropy from the East. An arrow pointing vertically downward indicates a radially directed anisotropic flow.

after the start of the flare. Both Figures 5 and 6 show that this phase of the flare event then gives way to a phase during which the anisotropy is directed from $\simeq 45°$ E. We interpret this latter phase as one in which there is a significant diffusive component of the cosmic ray current, $K\nabla \cdot U$, parallel to **B**, and which is being driven *towards* the Sun by positive gradient in U. Such an anisotropy has been predicted by Parker (1965), and by Forman (1970). Physical interpretations of these three phases are presented in Figure 7.

In Figures 3 and 4 the dotted lines are drawn at an angle of 45° to the east of the spacecraft-Sun line. It is apparent that in each case the anisotropy at very late times adopts a direction remarkably close to 45° east of the Sun. Further evidence to this end has been found from the analysis of data obtained by the Explorer 34 spacecraft (Allum *et al.*, 1971; Rao *et al.*, 1971), wherein, the electron and ionic anisotropies were observed at 40° and 41° E, respectively, during a long lived event observed in 1967, November, and other events show similar behaviour. Within the accuracy of our data, it seems reasonable to assert that the equilibrium anisotropy which is radially directed away from the Sun at early times, approximates the direction $\simeq 45° \pm 10°$ E of the radius vector at very late times. The fact that the $\simeq 45°$ E direction is adopted for each spacecraft, for each event, suggests that at very late times the cosmic ray current vector is accurately normal to **B**. We will return to this possibility later.

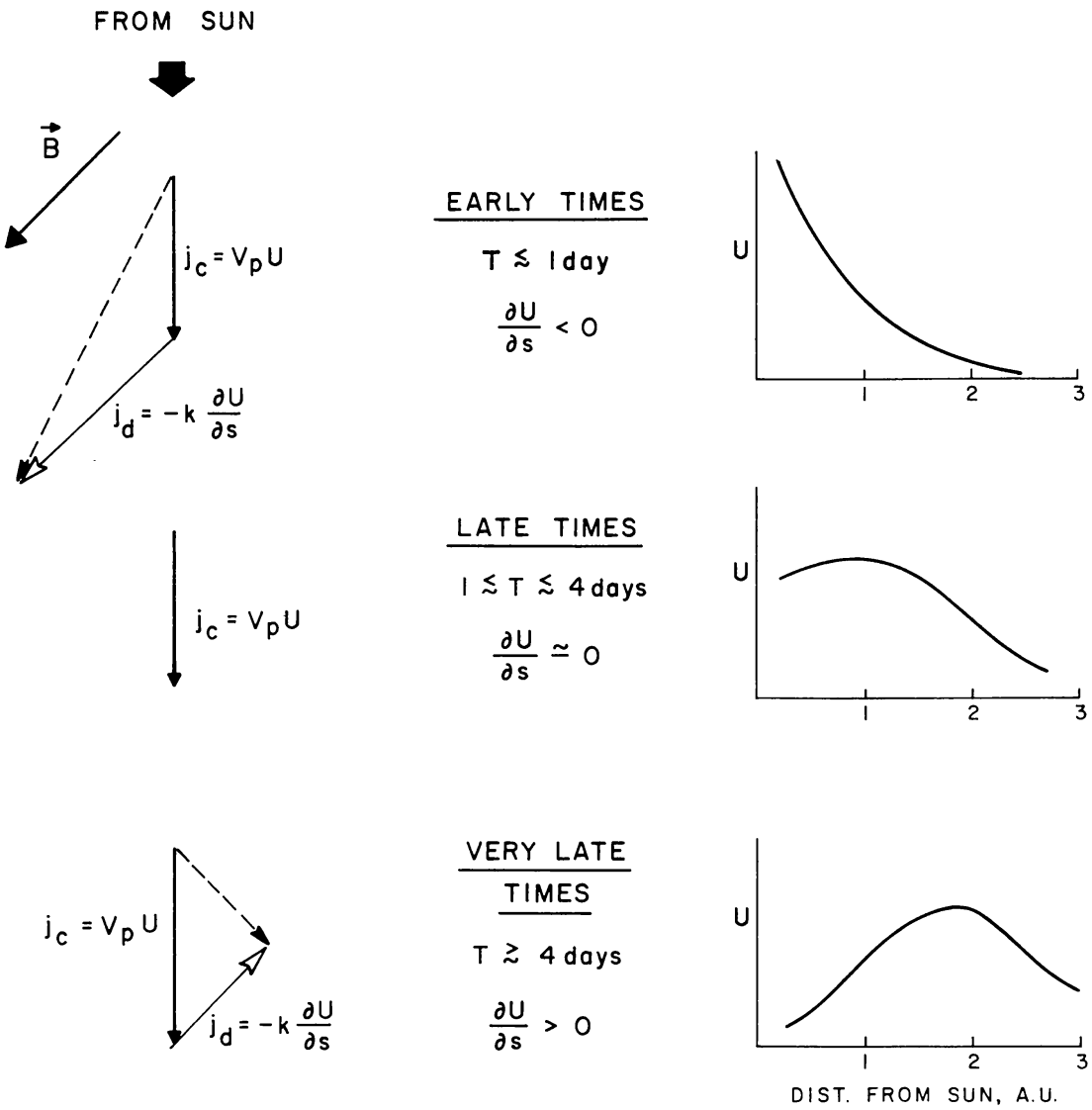

Fig. 7. The model for the evolution of the anisotropy of the cosmic ray solar flare effect. (a) Early times: a convective current, plus a diffusive current driven by a negative cosmic ray density gradient, as shown; (b) Late times: a convective current alone. There is no diffusive current since the cosmic ray density gradient is zero; (c) Very late times: a convective current, plus a diffusive current driven by a positive density gradient. All the above statements refer to the anisotropy observed at the orbit of Earth.

Writing the total anisotropy as the sum of convective, $\boldsymbol{\delta}_c$, and diffusive, $\boldsymbol{\delta}_d$, components, and following Forman (1970):

$$\boldsymbol{\delta} = \boldsymbol{\delta}_c + \boldsymbol{\delta}_d$$

where

$$\boldsymbol{\delta}_c = (2 + \alpha\gamma)\, V_p \hat{r}/v \tag{1}$$

and

$$\boldsymbol{\delta}_d = \frac{3}{v} \frac{K \cdot \nabla U}{U} \hat{\mathbf{B}}.$$

For a given cosmic ray spectrum, and given V_p, then $\boldsymbol{\delta}_c$ is determined unambiguously. The diffusive component $\boldsymbol{\delta}_d$ is not known, however, until ∇U and K are determined. In general, U will be a non-separable function of time and position, and will in fact change with time as a result of the very existence of $\boldsymbol{\delta}_c + \boldsymbol{\delta}_d$. It is therefore not immediately apparent how to determine $\boldsymbol{\delta}_d$ at late or very late times.

Consider, however, a tube of force in the interplanetary magnetic field. It is being convected outwards at the solar wind velocity. A cosmic ray initially in the tube of force will experience a guiding center drift $\mathbf{E} \times \mathbf{B}$, where $\mathbf{E} = 1/c \mathbf{V}_p \times \mathbf{B}$, and as a consequence, the guiding center of the particle remains on the original line of force (Ahluwalia and Dessler, 1962). As Forman (1970) has proposed, let us now consider the situation as seen from the frame of reference moving with the drift velocity $\mathbf{E} \times \mathbf{B}$. The irregularities in the magnetic field will now flow parallel or anti parallel to the magnetic vector direction with a velocity $V_{\parallel} = V_p \cos\theta$, where $\theta = \arctan \Omega R/V_p$, ($\Omega$ = solar angular rotation velocity; R = distance from Sun; V_p = solar wind velocity). Consequently, in this frame, the cosmic rays suffer convective removal at velocity $V_{\parallel}$ outwards along the magnetic field line.

The evidence, however, indicates that the direction of the cosmic ray anisotropy at very late times approximates 45° E, that is, it approximates the direction of $\mathbf{E} \times \mathbf{B}$. This indicates that at these times the convective current $V_{\parallel}\, U$ must be cancelled by a diffusive current $-K \partial U/\partial s$, where s is the distance measured outwards along the magnetic field line. That is, $\partial U/\partial s > 0$, so that the diffusive current is driven back towards the Sun. This indicates that the density gradient in the $\mathbf{E} \times \mathbf{B}$ frame of reference must be built up by the very presence of the convective anisotropy until it attains the asymptotic value $(\partial U/\partial s)_a = V_{\parallel}\, U/K$. At this time, the tendency for the cosmic ray anisotropy to increase the density gradient $\partial U/\partial s$ is exactly balanced against the tendency for the diffusive flow to destroy the gradient. That is, a complete state of equilibrium has been reached in the tube of force of interest. For this reason, we propose that the anisotropy from the East should also be called an 'equilibrium anisotropy'.

When this equilibrium pertains, the anisotropy seen from the spacecraft frame of reference will be that due to the $\mathbf{E} \times \mathbf{B}$ drift; it will be of amplitude

$$\delta = (2 + \alpha\gamma)\, V_p \sin\theta/v$$

and it will be normal to both $\mathbf{V}_p \times \mathbf{B}$ and $\mathbf{B}$.

4. The Dependence of the Cosmic Ray Density upon Heliocentric Longitude

We write the cosmic ray density* as $U(r, \psi, T, t)$. In this function, ψ is the heliocentric longitude of the intersection of the nominal Archimedes spiral through the point of observation with the solar surface. ψ is reckoned westward from a fixed point

* We speak of cosmic ray density here to remain consistent with the majority of the literature. In practice we measure the cosmic ray flux $\mathbf{F}$ averaged over all directions scanned by our detectors. Since the anisotropies are small ($\delta \lesssim 5\%$) at these times $\mathbf{F}$ and U are related by $\mathbf{F} = \mathbf{v}U/4\pi$.

on the rotating Sun. r, T, t are the distance from the Sun, the particle kinetic energy, and time respectively. Since the cosmic radiation remains associated with the same magnetic tube of force as it is convected out of the solar system, a cosmic ray population 'co-rotates' with the Sun. That is, the population remains associated with the same values of ψ throughout its lifetime in the solar system.

The rate of change of U with time, as observed by a spacecraft is given by:

$$\frac{dU}{dt} = \frac{\partial U}{\partial \psi}\frac{d\psi}{dt} + \frac{\partial U}{\partial r}\frac{dr}{dt} + \frac{\partial U}{\partial t}$$

where the term $\partial U/\partial t$ includes the effect of adiabatic decelleration. The second term is small, since dr/dt for the spacecraft is very small, so

$$\frac{dU}{dt} = \frac{\partial U}{\partial \psi}\frac{d\psi}{dt} + \frac{\partial U}{\partial t}. \tag{2}$$

Clearly, the two terms in (2) will add, or partially cancel depending on whether the observer is on the Eastern, or Western side of a cosmic ray population (Figure 8). Any discussion of the decay phase of a flare event observed from Earth, or a spacecraft, therefore requires knowledge of the dependence of U upon heliocentric longitude.

Figure 9 displays data obtained by three Pioneer spacecraft during a period which

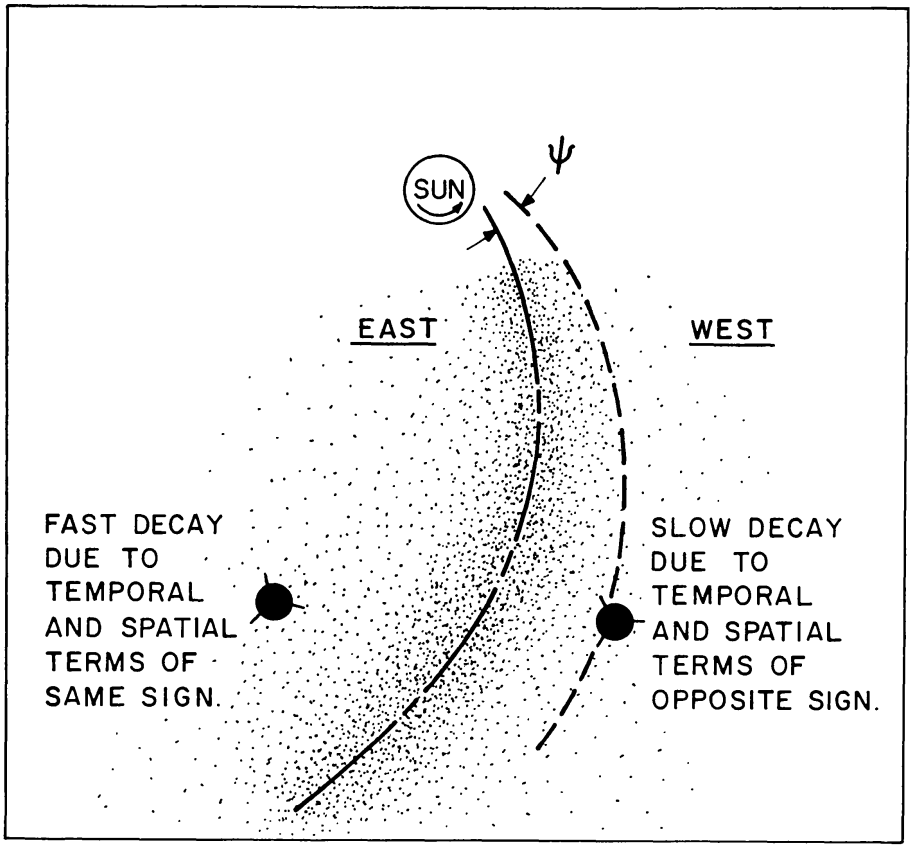

Fig. 8. A diagrammatic representation of the manner in which the position of an observer relative to the centroid of a cosmic ray population affects the nature of the decay phase of a flare effect.

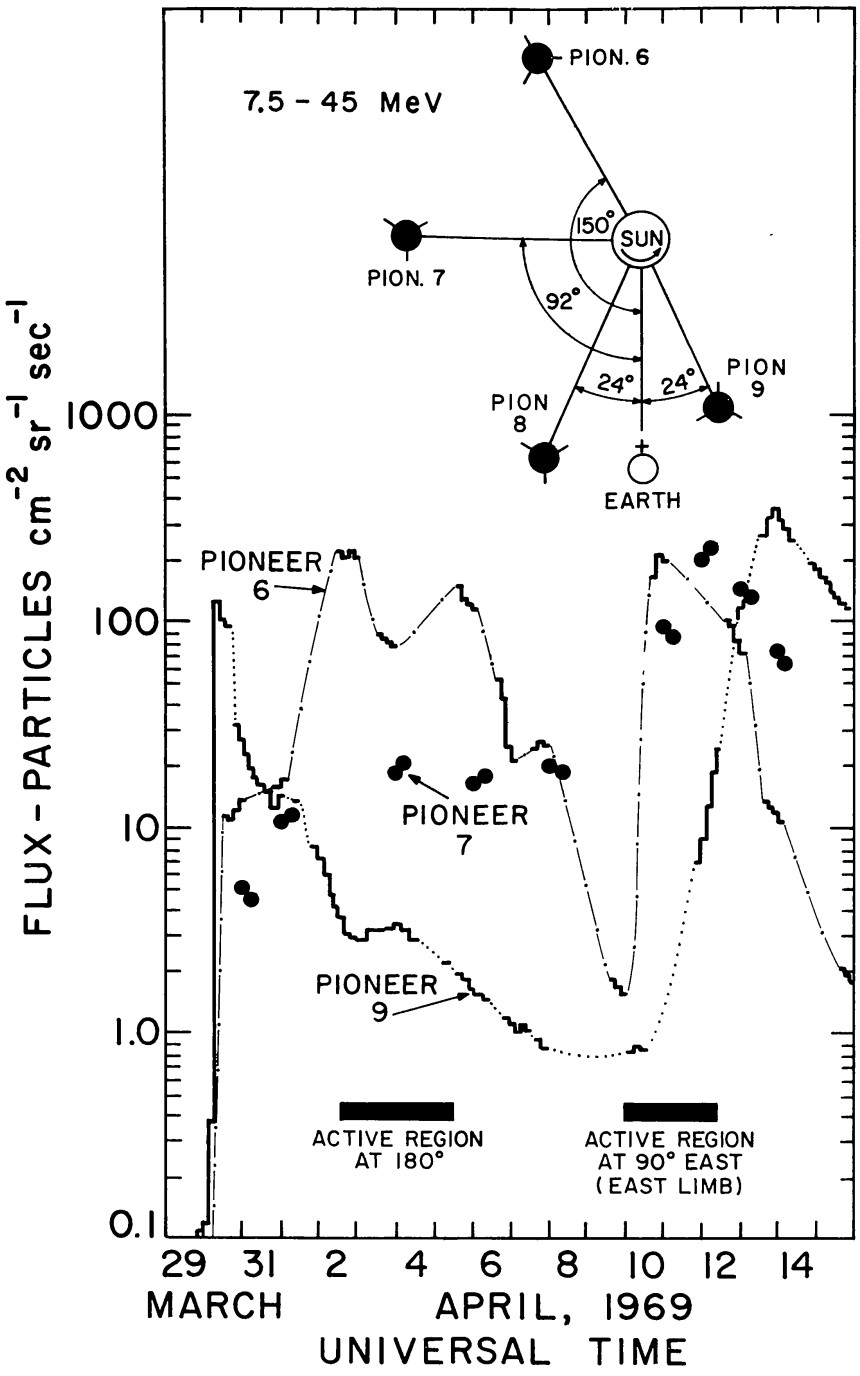

Fig. 9. Demonstrating the marked differences in the time variations of the solar cosmic ray flux observed at widely separated points in the solar system (see insert).

exhibited large cosmic ray fluxes of solar origin. Data were also obtained by Pioneer 8 during this period (see Figures 3 and 16). The totality of these data have been used to produce the graphs of the dependence of the omnidirectional cosmic ray flux upon heliocentric longitude which are presented in Figure 10.

Comparing the two periods in Figure 10, it should be noted that the curves for adjacent days are much closer together for 6–8 April than for 14–19 April, 1969. We

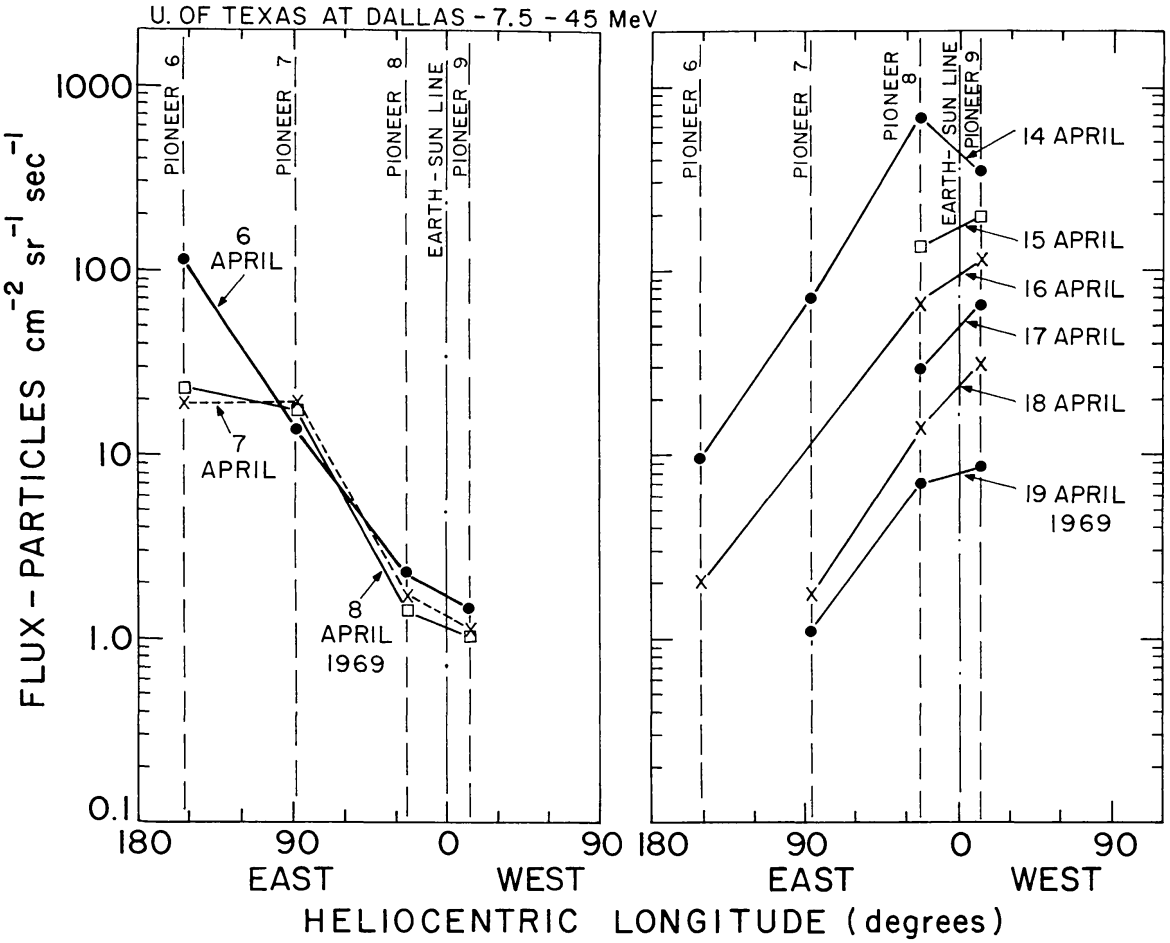

Fig. 10. The cosmic ray flux as a function of heliocentric longitude at very late times in two flare effects. The data for the period 6–8 April 1969 illustrate the situation when the observer is on the western side of the population, so that the increase in flux due to the corotation of the cosmic ray population partially cancels the depletion of the population due to convection and diffusion. The period 14–19 April illustrates the opposite situation, when the observer is on the eastern side of the population (see Figure 8).

attribute this to the fact that the spacecraft were on the Western side of the cosmic ray distribution for 6–8 April and on the Eastern side for 14–19 April. That is, in the latter case, the $\partial U/\partial t$ and $(\partial U/\mathrm{d}\psi).(\partial\psi/\mathrm{d}t)$ terms are both negative, while in the former the $\partial U/\partial t$ term is negative, while the $(\partial U/\mathrm{d}\psi).(\partial\psi/\mathrm{d}t)$ term is positive, thereby partially cancelling the $\partial U/\partial t$ term. That is, the 'co-rotation' of the cosmic ray population partially cancelled the temporal change for 6–8 April, resulting in a slow decay phase (also see Figure 16).

Comparing the curves in Figure 10, a similarity will be noted between the absolute values of the gradients of the flux over the ranges 90° E–24° E for 6–8 April, and 150° E–12° W for 14–19 April. Over both ranges, the data can be fitted by an exponential relationship $U^{-1}.\partial U/\partial\psi = 1/\psi_0$, where $\psi_0 = -28°$ for 6–8 April; and $\psi_0 = +34°$ for 14–19 April. The similarity of $|\psi_0|$ suggests that there may be a characteristic ψ_0 determined by the details of the process whereby the solar cosmic rays are

distributed in longitude. In both the cases illustrated in Figure 10 the parent flare injected cosmic rays at heliocentric longitudes such as to negate the possibility of study of the flux distribution near the center of the cosmic ray population. Clearly the distribution will not be the same exponential as noted above at such points in the cosmic ray population, however, it will be necessary to obtain further observations of the longitudinal gradient to resolve this question.

Futher consideration of Figure 10 indicates that the longitudinal gradient does not change radically with time during the decay phase of a particle population. Thus the gradient is essentially invariant for 150° E–12° W for the whole of the period 14–19 April, 1970. This indicates that the processes whereby cosmic rays are distributed in longitude at early times in a flare effect are no longer effective at late times ($T \gtrsim 2$ days from injection).

Note that at no place in the foregoing discussion we have assumed that the particle population is due to a single flare. Of the two cases considered, the data for the period 6–8 April clearly correspond to a particle population injected by more than one flare (*vide infra*), while those of 14–19 April correspond to a single injection. In the case of the 6–8 April data, cosmic radiation was initially released by a flare on 1969, March 30, which was 20° behind the western solar limb (Smerd, 1969). The Pioneer 6 data in Figure 9 indicates that there was at least one, and possibly two further injections during the period 2–5 April. These will be discussed in detail elsewhere (Bukata *et al.*, 1971). Since the latter flares were almost certainly associated with a single active center (McMath plage region 9994), this means that the several populations would be superposed upon one another, the maxima of the distributions being essentially coincident.

Clearly the foregoing conclusions, and the data in Figure 10 are strictly applicable to the events in question, alone. In the absence of other data, however, they provide approximate quantitative values and conclusions that will be applied to the flare effect in general.

5. The Decay Time Constant

On the basis of our earlier evidence demonstrating the dominance of convective removal processes over diffusion in the escape of $\simeq 10$ MeV cosmic rays from the solar system (McCracken *et al.*, 1967, 1968), Forman (1970) has shown that the cosmic ray density will vary with time as:

$$U = U_0 \exp - \left\{ \frac{2v_c}{r} \frac{(2 + \alpha\gamma)}{3} t \right\} \tag{3}$$

where the dependence of U on ψ as defined previously has been ignored.

From (2) then, we can write the observed variation as

$$\frac{\mathrm{d}U}{\mathrm{d}t} = \frac{\partial U}{\partial \psi} \frac{\mathrm{d}\psi}{\mathrm{d}t} - \frac{U}{\tau}$$

where

$$\tau = \frac{3r}{2v_c(2+\alpha\gamma)} \tag{4}$$

is the 'convective time constant'.

Approximating the total change in U to an exponential in which $dU/dt = -U/T$, where T is the observed time constant, then

$$-\frac{1}{T} = \frac{1}{U}\frac{\partial U}{\partial \psi}\frac{d\psi}{dt} - \frac{1}{\tau}$$

and if over a limited range of ψ, $U^{-1}\,\partial U/\partial\psi = 1/\psi_0$ as approximated earlier, then

$$\frac{1}{T} = \frac{1}{\psi_0}\frac{d\psi}{dt} + \frac{1}{\tau}. \tag{5}$$

In practice, we will find $20 \lesssim \tau \lesssim 40$ hr, $d\psi/dt = 0.54°\ \text{hr}^{-1}$, $\psi_0 \simeq \pm 30°$. As an example, then for $\tau = 20$ hr, the observed time constant $T = 14.3$ hr, or 31.2 hr, depending on whether the co-rotation effect reinforces, or partially cancels the convective decay term.

The anisotropy directed from the Sun, and from directions to the East of the Sun indicates convective removal of the cosmic rays from the solar system. Reference to Figure 7 indicates, however, that while the convective removal velocity is the plasma wind velocity, V_p, when the anisotropy is directed from the Sun, it becomes less than V_p when the anisotropy is from the East. Consequently, the convective decay time constant of the cosmic ray population, τ, will be greater than that computed on the basis of the full plasma wind velocity.

The effective convective velocity, v_c, defined as the radial component of the cosmic ray population's bulk velocity, can be derived in one of two ways:

(1) *On experimental grounds.* The observed anisotropy of amplitude δ is due to a bulk motion of the particle population, V_a, from a direction making an angle φ with the satellite-Sun line, (Figure 11), where δ is related to V_a by Equation (1) with V_p

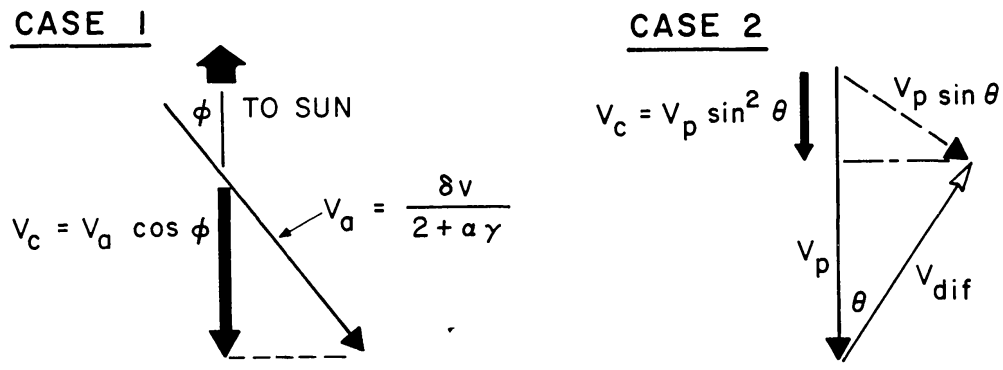

Fig. 11. Illustrating the derivation of the convective velocity, V_c.

replaced by V_a. Consequently the effective convective velocity, is given by

$$V_c = V_a \cos\varphi = \frac{\delta v \cos\varphi}{2 + \alpha\gamma}. \tag{6}$$

As an example, the Pioneer 9 data in Figure 2 exhibit a 4.3% anisotropy averaged over the period 17–20 April, inclusive, from the direction 45°E of the Sun. Table V suggests $\gamma = 3.5$ for this period, from which the mean energy of the data is 10.7 MeV. Using Equation (6), these data indicate an effective convective velocity of 152 km sec^{-1}. This is $\sim\frac{1}{2}$ of observed solar wind velocities. This suggests a factor of $\simeq 2$ increase may be expected in the value of the decay time constant, τ, as a result of the diffusive effects at late times in a flare event.

(2) *On theoretical grounds.* At late times, we have suggested that the anisotropy is normal to **B**, hence the effective convective velocity is given by

$$V_c = V_p \sin^2\theta. \tag{7}$$

For a typical value of $\theta = 45°$, $V_c = 0.5\,V_p$.

Further, writing $\eta = V_p/\Omega R = \operatorname{cotan}\theta$, then

$$V_c = V_p(1 + \eta^2)^{-1}$$
$$\frac{dV_c}{dV_p} = \frac{1 - \eta^2}{(1 + \eta^2)^2} \tag{8}$$

and we note that $dV_c/dV_p = 0$ for $\theta = 45°$. That is, the convective velocity is largely independent of the actual solar wind velocity for $V_p \simeq 450$ km sec^{-1} at orbit of Earth (when the anisotropy has become normal to **B**). This is illustrated in Figure 12, which shows that the convective removal velocity, V_c, lies in the range $200 < V_c < 215$ km sec^{-1} for $300 < V_p < 600$ km sec^{-1}. Figure 12 also illustrates the dependence of the convective velocity upon r. It is to be noted that V_c is asymptotic to the solar wind velocity V_p at large r.

Writing the convective decay time constant τ in terms of the effective convective velocity V_c, using Equations (4) and (6) gives

$$\tau = \frac{3r}{2v\delta\cos\varphi}. \tag{9}$$

Further, the theoretical values of V_c in Figure 12 have been used to calculate τ, using Equation (4), these results also being plotted in Figure 12. From Equations (4) and (9), and from Figure 12 the following conclusions can be reached regarding τ, the convective time constant:

(1) That with the passage of time, the evolution of the anisotropy from an anisotropy directed from the Sun, to one directed from the East, is accompanied by an increase in τ by a factor of ~ 2 near orbit of Earth.

(2) That at very late times ($T \gtrsim 4$ days), when the anisotropy is from the East, the time constant τ will be insensitive to variations in the solar wind velocity, V_p. At

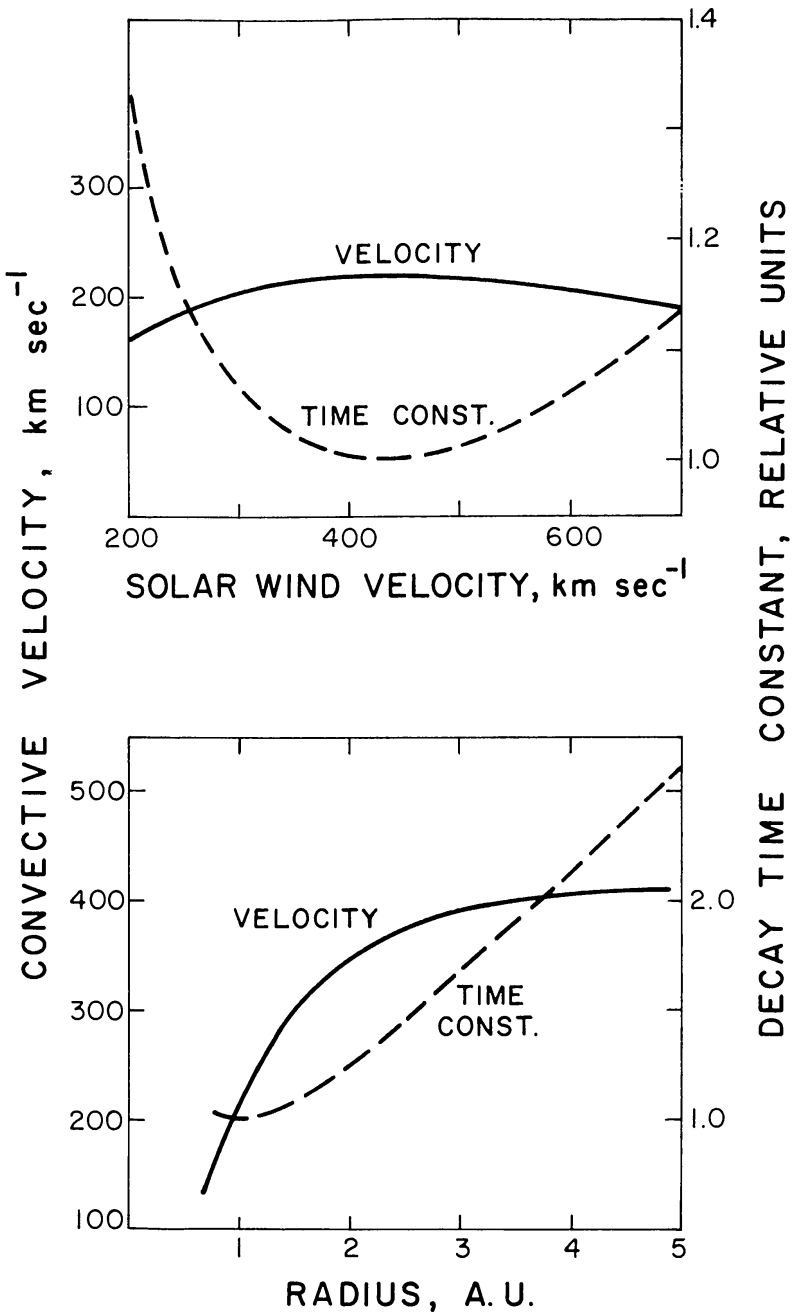

Fig. 12. The theoretical prediction as to the dependence of convective velocity, and the decay time constant τ as defined in Equation (4), upon solar wind velocity, and distance from the Sun.

somewhat earlier times ($1 \lesssim T \lesssim 4$ days), when the anisotropy is directly from the Sun, τ varies as the reciprocal of the solar wind velocity. These two cases are extremes. For these and intermediate cases, the time constant τ is expressable in terms of the parameters of the cosmic ray anisotropy.

(3) That the convective time constant varies with radial distance from the Sun. At times when the anisotropy is directed from the Sun, τ varies directly as r. At later times, the dependence upon r is weaker, τ increasing by a factor of 2 for r increasing from 1 to 4 AU.

(4) That the cosmic ray anisotropy, the e-folding angle ψ_0 of the heliocentric longitude gradient, and the time constant T of the decay observed by a spacecraft are related by

$$\frac{1}{T} = \frac{1}{\psi_0}\frac{\mathrm{d}\psi}{\mathrm{d}t} + \frac{2v\delta\cos\varphi}{3r}. \tag{10}$$

6. The Decay Time Constant-Experimental Results

Figures 2, 13, 14, 15, and 16 present the data obtained by Pioneers 8 and 9 during the major flares that occurred during the interval of interest. Table II summarises our current knowledge regarding the parent flares.

Inspection of the above graphs shows that the decay phase remains approximately

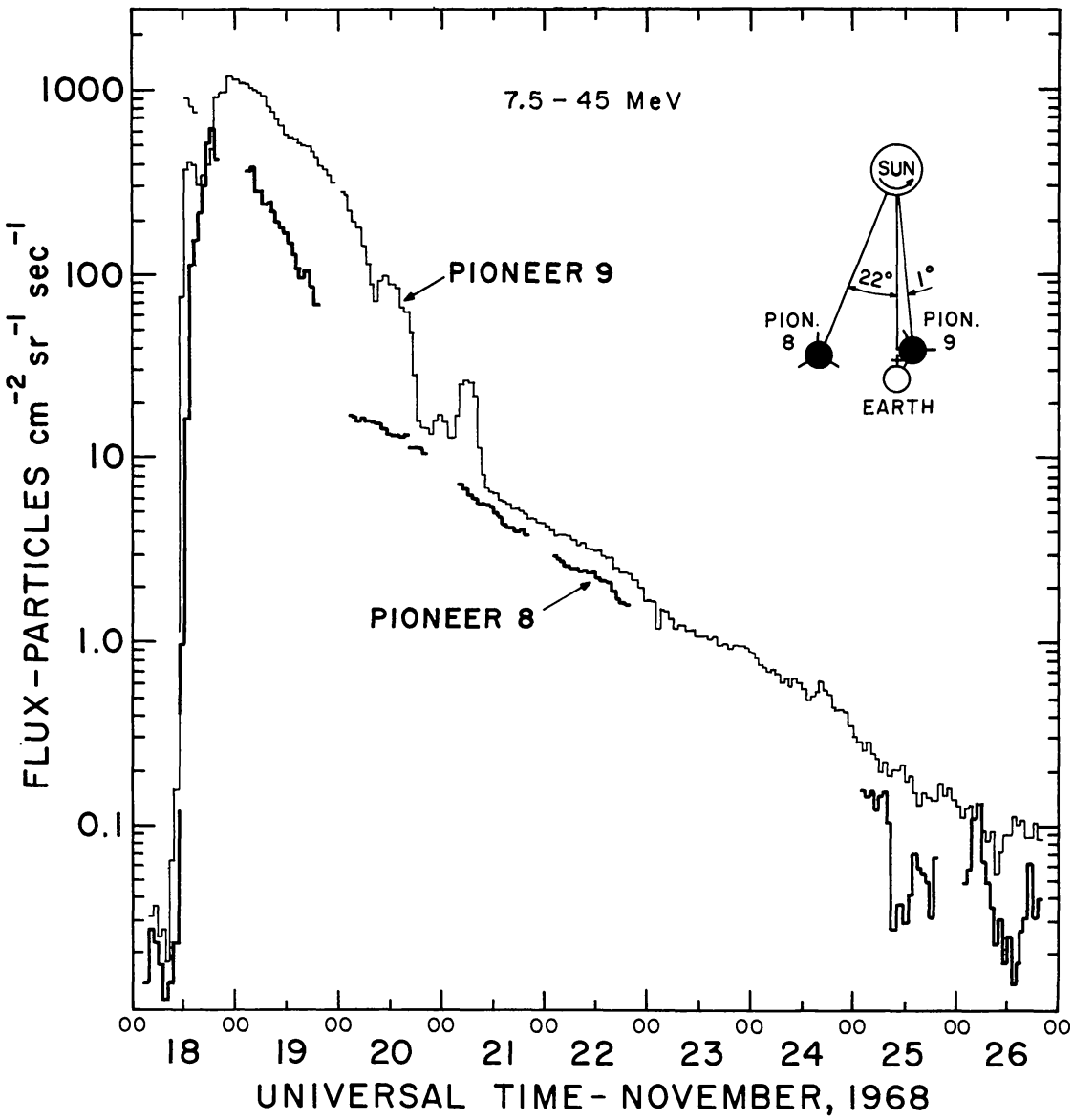

Fig. 13. The temporal variations of the 7.5–45 MeV cosmic ray fluxes observed by Pioneers 8 and 9 during the flare effect of 1968, November 18. The Pioneer 8 flux should be multiplied by a factor of 1.7.

TABLE II

The parent flares responsible for the cosmic ray increases discussed in this paper. [a]

Date	Flare onset UT	Importance	McMath plage region	Flare coordinates		S/C Long	
						P8	P9
1968, 18 Nov.	1017	1B	9760	N21	W87	E22	W1
1968, Dec. 2	2116	3N	9802	N18	E80	E22	W2
1969, Mar. 12	1738	2B	9966	N12	W80	E24	W15
1969, Mar. 30	0248	?	9994	N19	W111	E24	W24
1969, Apr. 11		?			≃ E45	E25	W32

[a] The column 'S/C Long' lists the longitudes of the feet of the nominal Archimedes spirals through the spacecraft relative to the parent flare. The identification for the 30 March 1969 flare is based on Smerd (1970). There was a gap in the flare patrol at the time of the 11 April 1969 event. The 'Flare coordinate' listed in this case is that of a very active centre which was on the solar disc at the time. The cosmic ray data, and in particular the gradient data in Figure 10, are in good accord with this assignment.

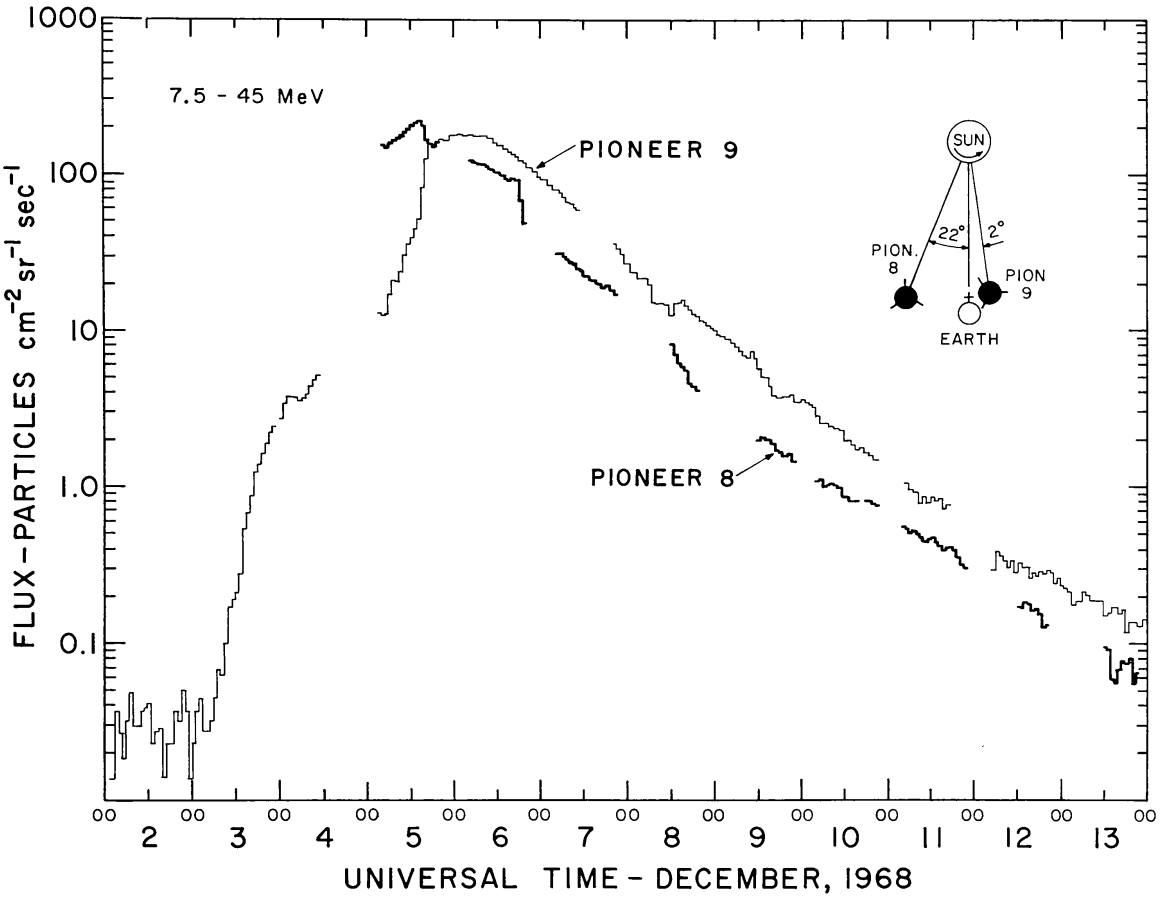

Fig. 14. The temporal variations of the 7.5–45 MeV cosmic ray fluxes observed by Pioneers 8 and 9 during the flare effect of 1968, December 3. The Pioneer 8 flux should be multiplied by a factor of 1.7.

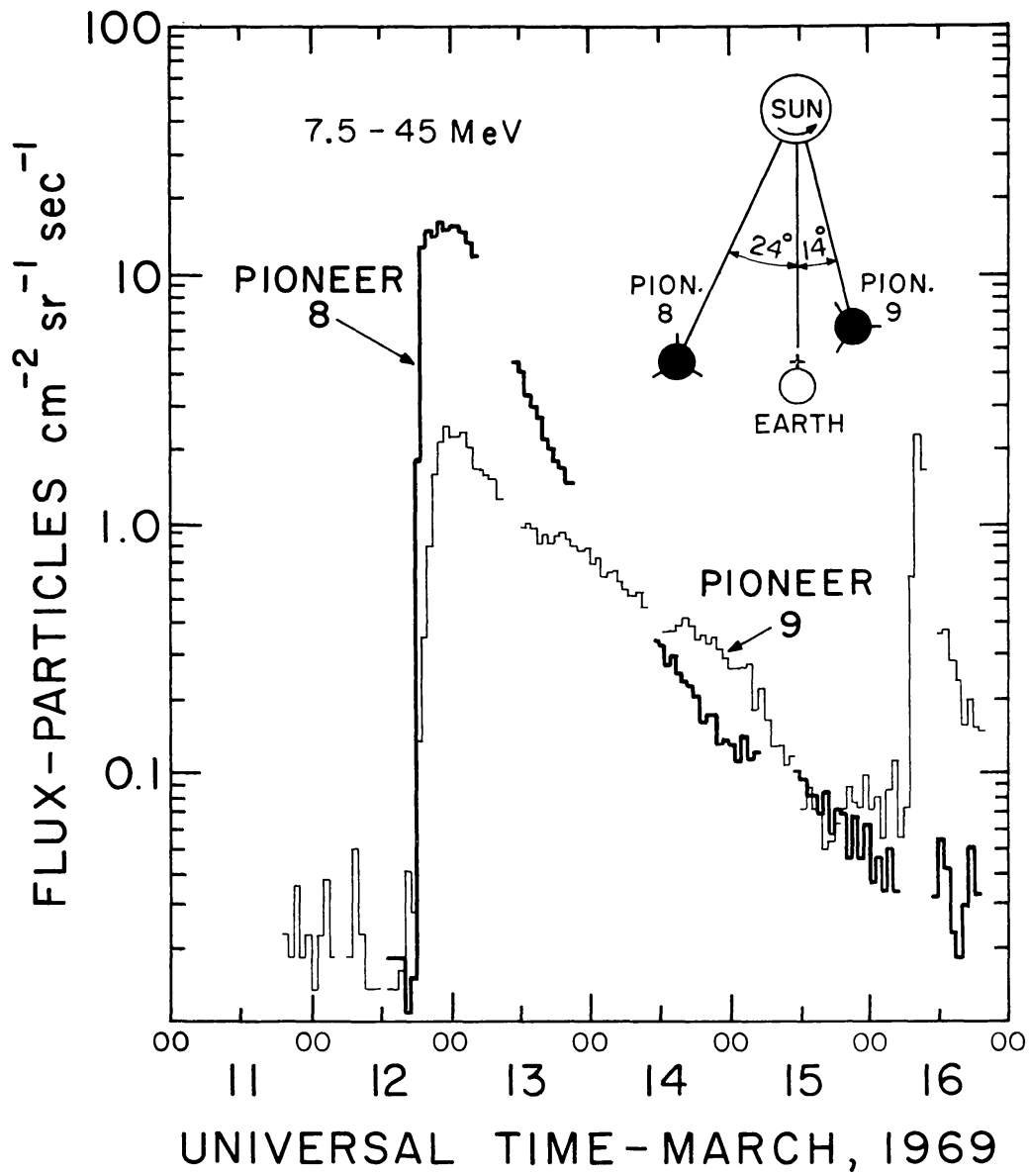

Fig. 15. The temporal variations of the 7.5–45 MeV cosmic ray fluxes observed by Pioneers 8 and 9 during the flare effect of 1969, March 12. The Pioneer 8 flux should be multiplied by a factor of 1.7.

exponential over periods of many days, and over 2–4 orders of magnitude changes in particle flux. There are short term fluctuations in the time constant (e.g., Pioneer 9 data in Figure 2), some of which correlate with changes in anisotropy amplitude and phase, as will be discussed later.

Table III summarizes the anisotropy and longitudinal gradient data that are presently at our disposal for late times ($T \gtrsim 4$ days) in four flare effects. From these data we have calculated the convective time constant τ from Equation (9), and the time constant that Equation (5) predicts for a spacecraft, T_{calc}. The observed time constants T_{obs} are also listed. Figure 17 shows $1/T_{obs}$ plotted against $1/T_{calc}$. The data in the figure have a correlation coefficient of 0.77 ± 0.10, and a mean regression coefficient of 0.9. This high degree of correlation in the data, and the closeness of the

TABLE III

Summary of the calculation of decay time constants, and their comparison with the observed values [a]

Period	Spacecraft	r (AU)	δ (%)	φ (degrees)	ψ_0 (degrees)	τ (hours)	T_{calc} (hours)	T_{obs} (hours)
1968, Nov. 21–22	Pion. 8	1.00	4.3 ± 0.4	40°E	+(60) [b]	42.5 ± 5 5.6	$30.8 \pm$ 2.8	28 ± 3
1968, Nov. 22–24	Pion. 9	1.00	5.5 ± 0.5	53°E	−(60) [b]	$34.4 \pm$ 4.3	$49.9 \pm$ 9.4	35 ± 5
1968, Dec. 8–10	Pion. 8	1.00	6.3 ± 0.4	45°E	+ 55° [b]	$31.5 \pm$ 2.8	$24.1 \pm$ 1.6	27 ± 4
1968, Dec. 9–10	Pion. 9	0.99	3.1 ± 0.5	25°E	+ 55° [b]	47.9 ± 10.7	$32.4 \pm$ 4.8	22 ± 2
1969, Apr. 6–8	Pion. 8	1.00	7.1 ± 0.5	45°E	− 28°	$27.8 \pm$ 2.8	60.0 ± 14.5	~ 120
	Pion. 9	0.75	2.5 ± 0.5	45°E	− 28°	60.6 ± 16.8	−156 to +260	~ 83
1969, Apr. 7–20	Pion. 8	1.00	3.3 ± 0.4	40°E	+ 34°	$55.3 \pm$ 9.5	$29.4 \pm$ 2.5	28 ± 2
	Pion. 9	0.75	4.2 ± 0.3	42°E	+ 34°	$33.8 \pm$ 3.5	$22.0 \pm$ 1.4	30 ± 4

[a] The columns are as follows: r = distance from Sun; δ = anisotropy amplitude; φ = anisotropy phase; ψ_0 = e-folding angle for cosmic ray gradient; τ = calculated convective time constant; T_{calc} = calculated time constant at spacecraft; T_{obs} = observed time constant at spacecraft. The anisotropy data refer to the energy range 7.5–21.5 MeV, while the observed time constant is calculated from the 7.5–45 MeV counding rate data.

[b] The e-folding angles were not directly measured. See text.

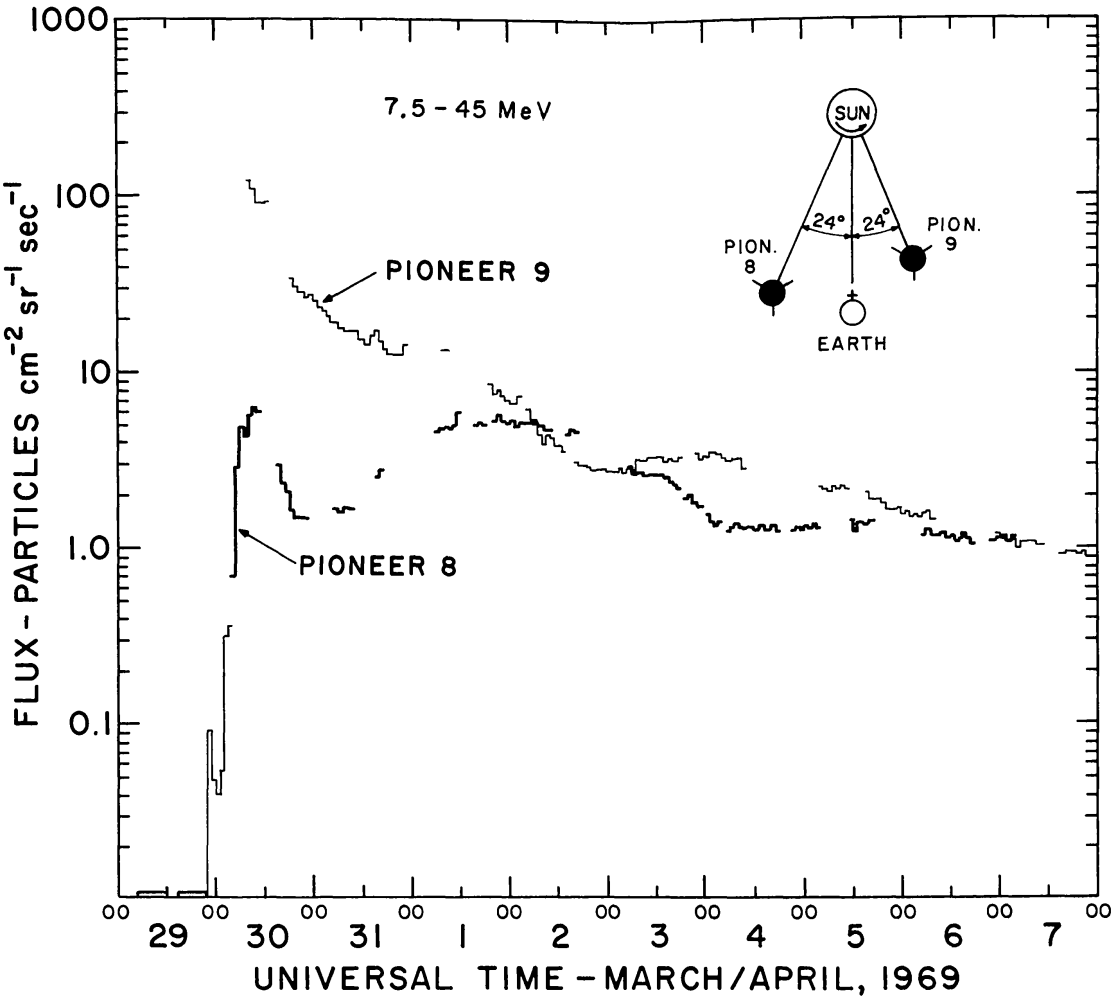

Fig. 16. The temporal variations of the 7.5–45 MeV cosmic ray fluxes observed by Pioneers 8 and 9 during the flare effect of 1969, March 30. The Pioneer 8 flux should be multiplied by a factor of 1.7.

mean regression coefficient to unity, indicate that Equation 10 accurately describes the relationship between the anisotropy, the longitudinal gradient, and the decay time constant of a flare effect.

With regard to the data in Table III, it must be noted that definitive values of ψ_0 are only available for the two 1969, April, flare events (see previous section of this paper). We have consequently estimated values of ψ_0 for the two earlier flare effects using Pioneer 8 and 9 data as follows.

(1) *1968, November 21–24.* In this event, the absolute value of the fluxes at the two spacecraft, Pioneers 8 and 9, were approximately the same at about November 21, the fluxes thereafter decreasing more rapidly with time at Pioneer 8 than at Pioneer 9. We have therefore assumed a cosmic ray density distribution with a maximum midway between the two spacecraft, with $\psi_0 = \pm 60°$. The satisfactory nature of the correlation in Figure 17 is insensitive to this assumption: Thus $\psi_0 = \infty$ at both spacecraft results in an equally satisfactory correlation.

(2) *1968, December 8–10.* In this case, the Pioneer 9 flux exceeded that at Pioneer 8

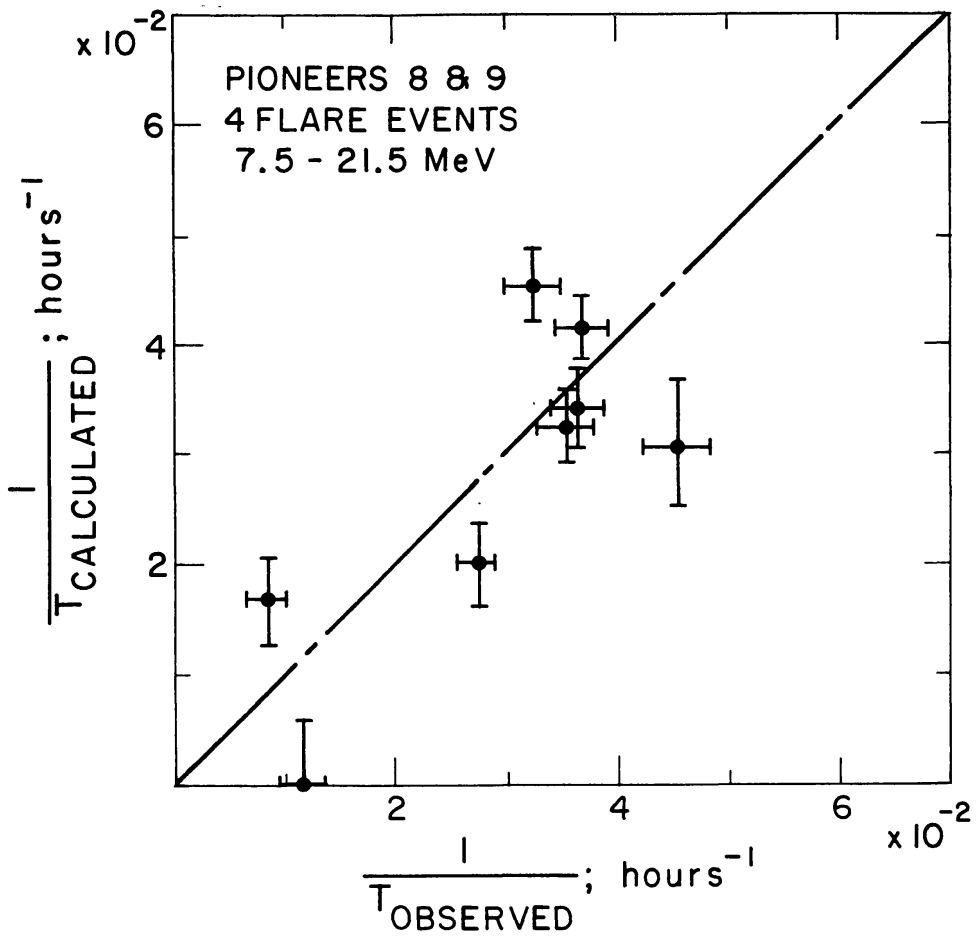

Fig. 17. Illustrating the agreement between the observed time constant, and that calculated from the characteristics of the anisotropy, and the cosmic ray distribution in heliocentric longitude.

by a factor of $\simeq 1.6$. We have therefore assumed that this is due to a gradient of e-folding angle 55°. The correlation in Figure 17 is not dependent upon this assumption.

It should be noted, however, that the good correlation in Figure 17, while insensitive to the assumed values of ψ_0 for the first two events, is strongly dependent on the values of ψ_0 for the 1969 April events (for which ψ_0 are well known). That is, the gradients in the region of space sampled by Pioneers 8 and 9 were much stronger in the latter events. This, in itself, is a crucial factor that has permitted the use of these events to demonstrate the validity of Equation 10 over a wide range of ψ_0. We note that apart from this, the fact that all the points in Figure 17 lie on or near the line of unity slope is evidence of the validity of the equation.

The several time decay curves, Figures 2, 13, 14, 15, and 16, make it clear that there are short term fluctuations superposed upon the long term decay of a flare effect. For example, by fitting an exponential to 24 hr segments of the Pioneer 9 data for April 16–20, time constants of $19 < T_{obs} < 50$ hours are obtained, as is demonstrated in Table IV. Furthermore, Figure 3 shows that fluctuations were also observed in the anisotropy observed by Pioneer 9 during this period. Table IV and Figure 18 examine

TABLE IV

Summary of the day to day changes in the anisotropy, and decay time constant during 16–20 April, 1969, as observed by Pioneer 9. [a]

Day	δ (%)	φ (Degrees)	τ (Hours)	T_{calc} (Hours)	T_{obs} (Hours)
1969, Apr. 16	1.5 ± 0.11	69° E	202 ± 19	47.8 ± 1.1	43 ± 3
1969, Apr. 17	4.3 ± 0.2	67° E	62.1 ± 4.1	31.2 ± 1.2	27 ± 2
1969, Apr. 18	5.5 ± 0.2	24° E	20.8 ± 1.1	15.7 ± 0.7	19 ± 1
1969, Apr. 19	3.4 ± 0.5	41° E	40.7 ± 8.4	24.8 ± 3.2	32 ± 2
1969, Apr. 20	4.4 ± 0.6	43° E	32.4 ± 6.2	21.4 ± 2.5	50 ± 4

[a] The tabular quantities are defined as in Table III. In calculating T_{calc}, we have taken $r = 0.75$ AU and $\psi_0 = +34°$.

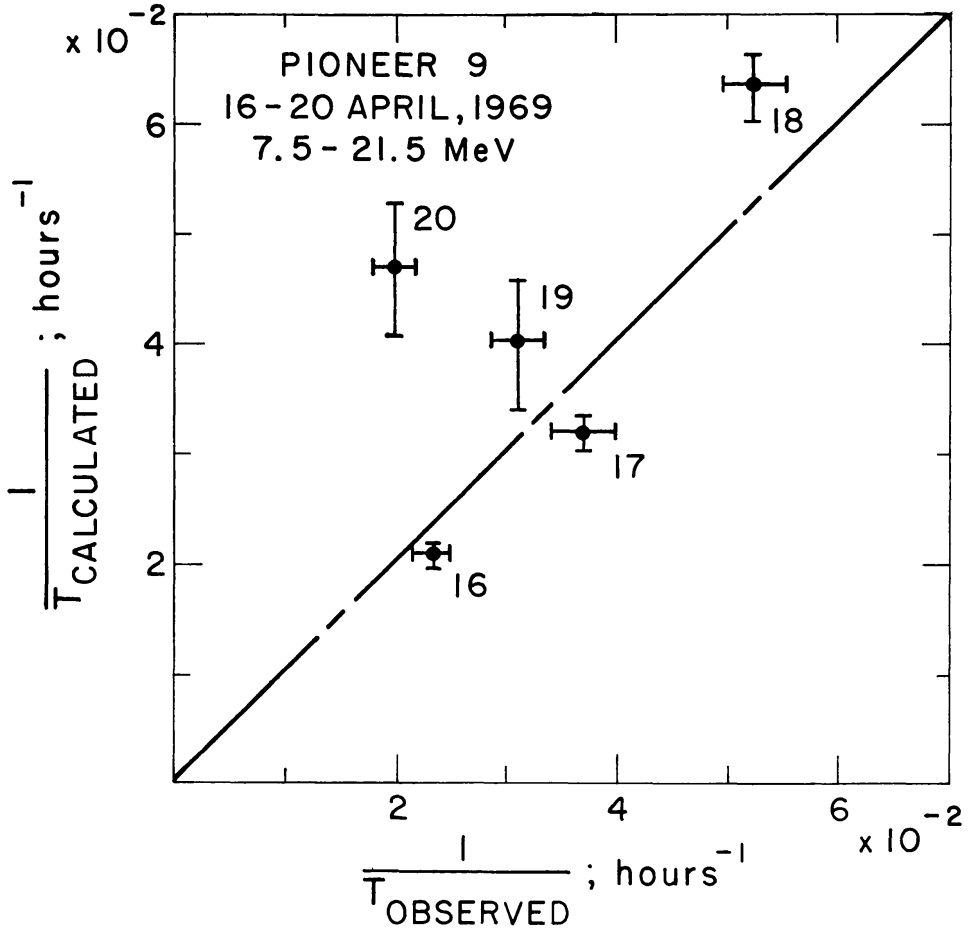

Fig. 18. Illustrating the validity of Equation (10) in the case where ψ_0 is invariant. That is, this illustrates the interdependence of the decay time constant and the characteristics of the anisotropy.

the correlation between these phenomena. Thus assuming $\psi_0 = 34°$ to be the e-folding angle throughout the interval April 16–20, the time constant T_{calc} has been computed from the properties of the anisotropy. It is clear from Figure 18 that the calculated values are in agreement with observations.

From the foregoing, it is evident that the anisotropy, and the density gradients in heliocentric longitude, are the quantities that determine the decay time constant. The fact that the anisotropy does vary with time during the decay phase (e.g. Table IV, or Figure 16 of Allum *et al.* (1971)), temporarily deviating from the 45° E direction, is presumably due to the spacecraft sampling cosmic rays in a tube of force in which the radial gradient is insufficient to balance the convective removal parallel to **B**. The fact that the deviations of the anisotropy phase angle, and decreased time constant on April 18, 1969 (Figure 2) are associated with an increased solar wind velocity is probably significant in this regard.

7. The Cosmic Ray Energy Spectrum

Pioneer 8 and 9 both provide 6 point spectral information in the energy range 5–50 MeV. For each of the flare effects in Figures 2, 13, 14, and 16, we have averaged the data over complete calendar days, to yield daily average spectra throughout the flare event, for each spacecraft. The observed counting rates and the widths of the spectral windows have been corrected for (a) overlying absorber, and (b) the effects due to the FWHM of the pulse height distribution of the detector being comparable to the lower energy window widths. The absolute energy calibration corresponding to each window has been verified (and corrected in the case of Pioneer 8) using the results from periodic calibration with an Am^{241} source.

Typical spectra obtained in this manner are displayed in Figure 19 for the decay phase of the flare effect of 1968, December 2. Of note, is the absence of any noticeable change in spectral slope over the three days in question. We observe this to be the normal situation at late times ($T \gtrsim 2$ days) in the flare effects, that have been studied to date. Nevertheless, marked differences in spectral character are noted when the spectra obtained during the decay phases of different flares are compared, as is demonstrated in Figure 20.

To characterize these differences in spectral character, we have fitted a simple power law $\mathrm{d}j = j_0 E^{-\gamma}\,\mathrm{d}E$ to each spectrum. In fact, the fit is not perfect in the lowest energy channel, however, this is of no consequence insofar as the present discussion is concerned. The values of γ for five flare effects are listed in Table V. For each day for which a spectral exponent is given, we have also computed the longitude of the spacecraft relative to the centroid of the cosmic ray population, which is assumed to have been injected onto the nominal Archimedes spiral line of force that passes through the parent flare. That is

$$\psi' = \xi_{sc} - \left[\xi_f + \frac{\mathrm{d}\psi}{\mathrm{d}t}\cdot T - \Delta\xi_A\right] \tag{11}$$

$$= \xi_{sc} - [\xi_f + 14.2°\ T - 57°] \tag{11'}$$

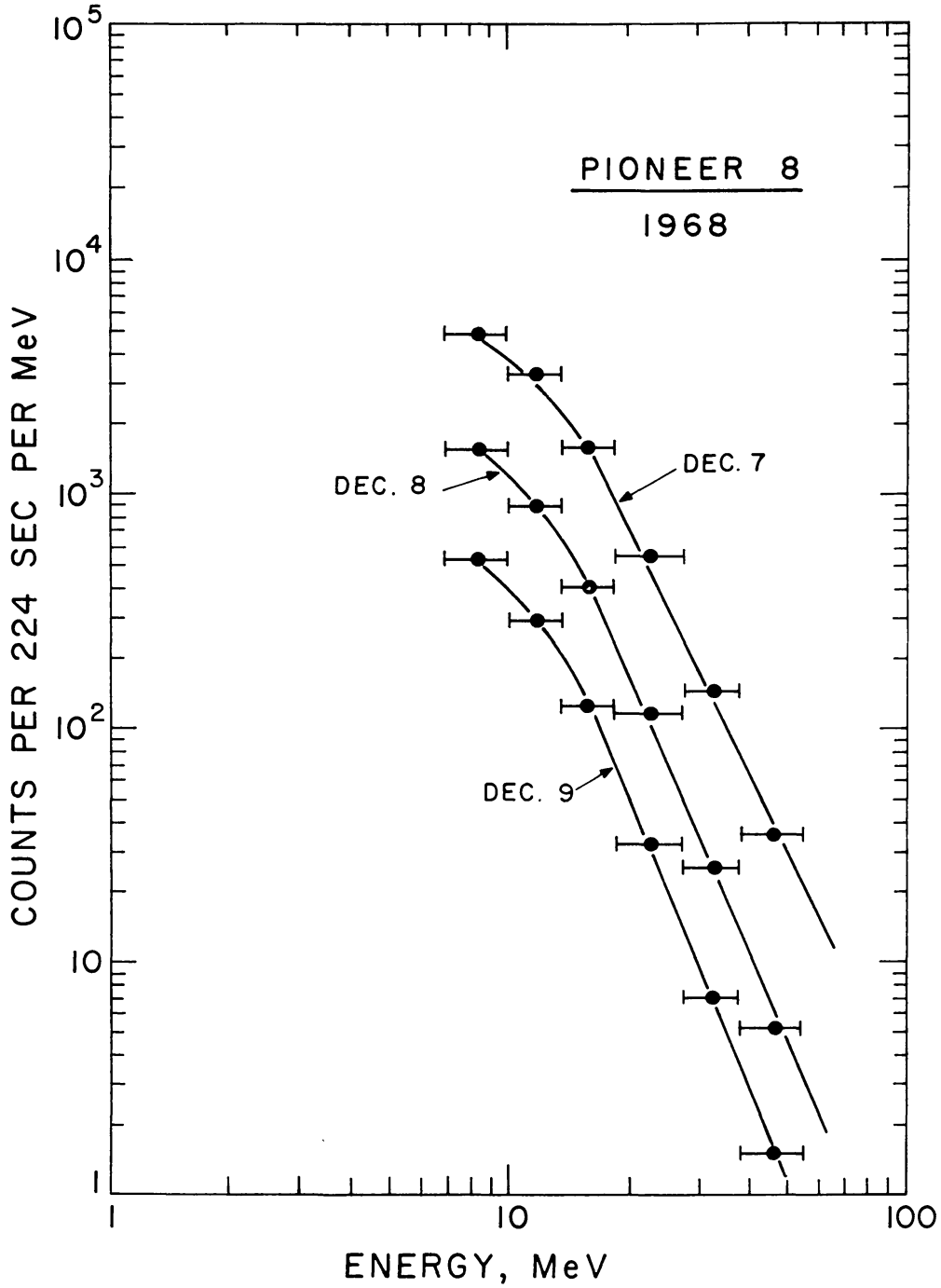

Fig. 19. Illustrating the insensitivity of the cosmic ray spectrum to the passage of time at late and very late times in the solar flare effect. The standard errors due to counting rate statistics are smaller than the graphical symbols.

where ξ is heliocentric longitude relative to the central meridian of the Sun as seen from Earth; T is time (in days) since the flare; $\Delta\xi_A$ is the longitude difference for the nominal spiral line that makes an angle of 45° with the radius vector at orbit of Earth; $d\psi/dt$ is the solar rotation rate (degrees per day); and the subscripts f and sc represent 'flare' and 'spacecraft'.

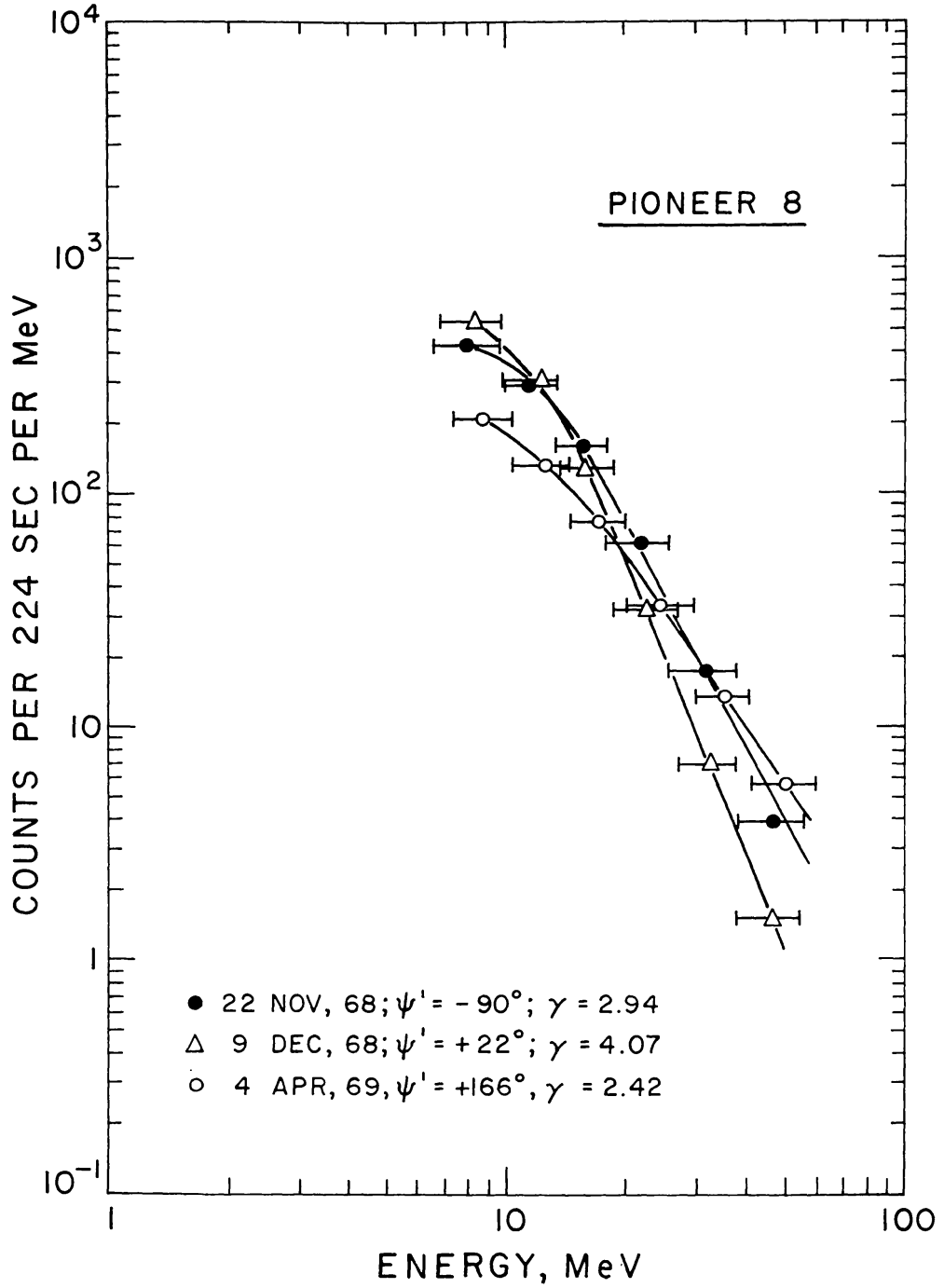

Fig. 20. Illustrating the dependence of the cosmic ray spectrum upon the population longitude, ψ', of the observer.

In Figure 21 the spectral exponent is plotted against ψ' for late times in the decay phase of the flare events listed in Table V. The data for $0 < T < 4$ days for the 1969, March 30 event and the data for the short lived 1969, March 12 event have been omitted from this graph, since there is considerable evidence that the flare event of 1969, March 30 was greatly different from the majority of flare effects (Bukata *et al.*, 1971). Subsequent to $T=4$, the data for this event have been used. It appears

TABLE V

The spectral exponents, γ, for the energy spectra in the 5–50 MeV energy range, for the five flare events and for both Pioneers 8 and 9.[a]

Date of flare	T	ψ_8'	γ_8	ψ_9'	γ_9
18 Nov. 1968	+ 3	− 76	3.13 ± 0.06	− 53	3.37 ± 0.04
	+ 4	− 90	2.94 ± 0.05	− 67	3.28 ± 0.06
	+ 5			− 81	2.90 ± 0.09
	+ 6			− 96	2.76 ± 0.13
2 Dec. 1968	+ 5	50	3.43 ± 0.03	74	3.19 ± 0.02
	+ 6	36	3.91 ± 0.11	60	3.67 ± 0.03
	+ 7	22	4.07 ± 0.19	46	4.08 ± 0.06
	+ 8	8	3.72 ± 0.21	32	3.86 ± 0.11
12 Mar. 1969	0		2.14 ± 0.04		1.78 ± 0.09
	1		3.08 ± 0.05		2.59 ± 0.07
	2	?	3.10 ± 0.27	?	2.47 ± 0.12
	3		2.60 ± 0.30		2.62 ± 0.18
30 Mar. 1969	+ 5	166	2.42 ± 0.10	−145	1.29 ± 0.05
	+ 6	152	2.53 ± 0.10	−160	1.89 ± 0.07
	+ 7	138	2.84 ± 0.13	−174	2.03 ± 0.08
	+ 8	124	2.88 ± 0.20	172	2.48 ± 0.12
	+ 9			157	2.48 ± 0.12
	+10			143	2.79 ± 0.13
11 Apr. 1969	0	35	3.82 ± 0.03	92	
	+ 1	21	3.81 ± 0.03	78	3.18 ± 0.05
	+ 2	7	4.34 ± 0.07	64	3.33 ± 0.08
	+ 3	− 8	4.12 ± 0.08	49	3.29 ± 0.13
	+ 4	− 22	4.10 ± 0.11	35	3.59 ± 0.35

[a] ψ_8' and ψ_9' are the longitudes of the feet of the nominal Archimedes spiral through the two spacecraft reckoned relative to the current position of the region of the Sun where the flare occurred. That is, these angles are the longitudes of the spacecraft relative to the centroid of the cosmic ray populations injected by the parent flare. γ_8 and γ_9 are the spectral exponents for the two spacecraft.

that the radiation observed subsequent to that time originated in another one, or two flares on the non-visible hemisphere (Bukata *et al.*, 1971).

Examination of Figure 21 shows that there is a remarkably well defined relationship between the spectral exponent and the population longitude, ψ. The graph indicates that the observer who is near the Archimedes spiral through the parent flare observes a steep spectrum, with $\gamma = -4$ to -5, while an observer less favourably situated relative to the flare sees a considerably harder spectrum. We stress that the evidence, to date, only refers to late or very late times in the flare effect ($T \gtrsim 2$ days).

One implication of the dependence of γ upon ψ is that the variation of cosmic ray flux with heliocentric longitude, and consequently the e-folding angle ψ_0, must be functions of particle energy. Thus Figure 21 suggests that the spatial and energy dependence of the isotropic cosmic ray flux is given by

$$F(\psi, E) = F_0 f(\psi) E^{-[\gamma_0 - k\psi]} = F_0 f(\psi) E^{-\gamma}$$

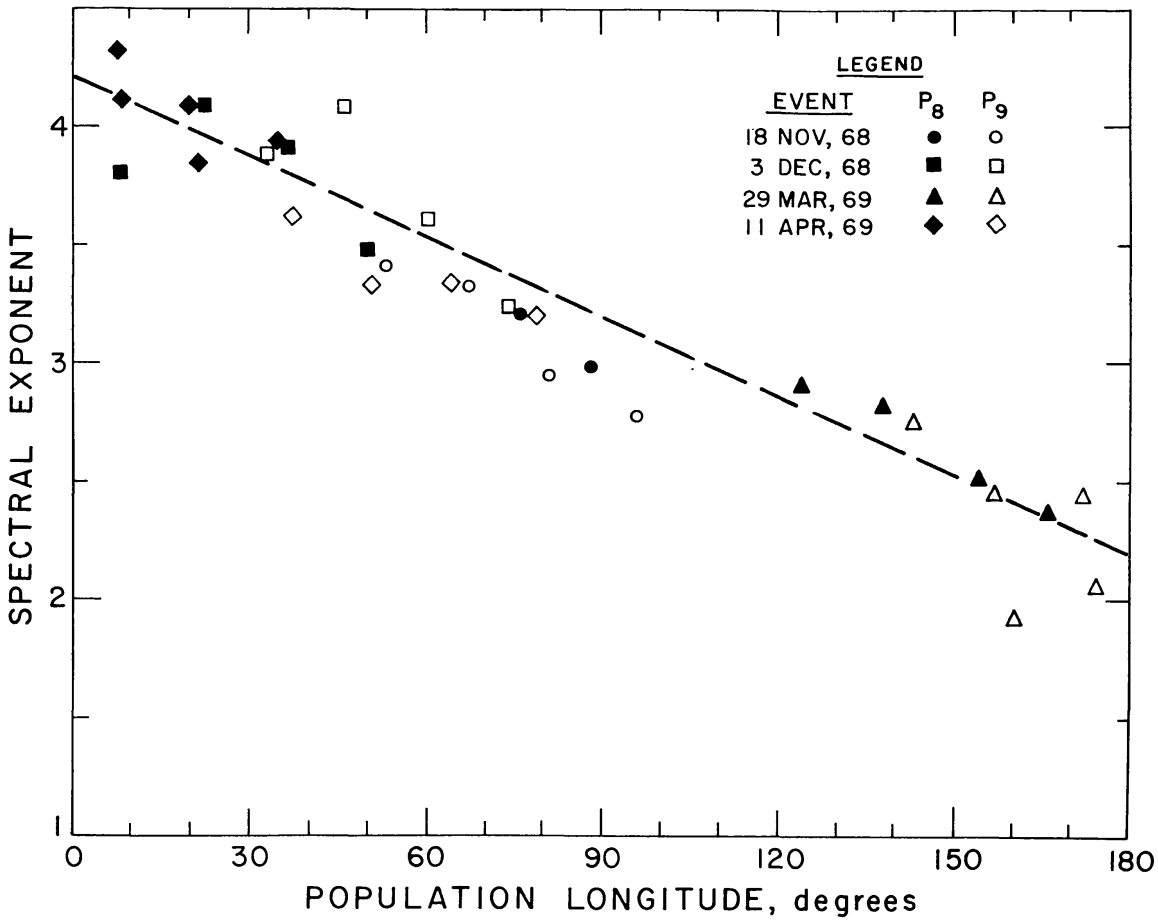

Fig. 21. The observed dependence of spectral exponent, γ, upon the position of the observer relative to the centroid of the cosmic ray population injected by a flare.

where γ_0 and k are constants of the population of solar flare effects under consideration. Figure 21 indicates that $\gamma_0 = 4.25$ and $k = 1.1 \times 10^{-2}$ deg^{-1}.

Differentiating, and dividing by $F(\psi, E)$, the e-folding angle $\psi_0(E)$ is obtained to be

$$\frac{1}{\psi_0(E)} = -\frac{1}{F}\frac{\partial F}{\partial \psi} = -f'/f - k \log_e E. \tag{12}$$

If $\psi_0(E)$ is known at energy E_0, then the functional dependence of $\psi_0(E)$ on energy is given by

$$\frac{1}{\psi_0(E)} = \frac{1}{\psi_0(E_0)} + k \log_e (E_0/E).$$

For the observed values of $\psi_0 = 30°$ at $\psi = 90°$ and $E_0 = 10$ MeV, this becomes

$$\frac{1}{\psi_0(E)} = \frac{1}{30} + 1.1 \times 10^{-2} \log_e\left(\frac{10}{E}\right). \tag{13}$$

As discussed previously, our observations have all indicated that the 'co-rotation' term $(\partial u/\partial\psi)\cdot(\mathrm{d}\psi/\mathrm{d}t)$ in Equation (2) is always numerically less than the convection term at $\simeq 10$ MeV. Further, the convection time constant τ is independent of energy (see Equation (4)) provided that γ is constant over the energy range of interest. Consequently, since Equations (12) and (13) show that ψ_0 decreases with decreasing energy, and that the absolute magnitude of the co-rotation term therefore increases with decreasing energy, this must ultimately cause $T=\infty$ (for an observer on the Western side of a particle population). For lower energies than this, the time constant in Equation (5) will be negative, indicating that the solar cosmic ray flux will *increase* with time if the observer is to the west of the centroid of a particle population. Such behaviour is observed for $E<3$ MeV for the period 6–9 April, 1969, as is discussed by Bukata *et al.* (1971). Thus it is shown that calculations based on Equations (12) and (13) predict that the decay time constant was infinite at 1.7 MeV during the above period. This prediction is in general accord with the independent observations of the time profiles at energies between 0.7 and 50 MeV.

Reference to Equation (4) shows that the convective time constant, τ, is sensitive to the exponent, γ, of the differential energy spectrum. Figure 21 shows therefore that τ will depend upon the position of the observer relative to the centroid of the cosmic ray population injected by the flare, that is, it will depend upon ψ. Reference to Equation (5) indicates that the manner in which the observed time constant, T, depends upon the population longitude, ψ, will be determined by both this dependence of τ on ψ, and by any dependence of ψ_0 (the instantaneous value of the e-folding angle) upon ψ. If anything, we expect ψ_0 to increase with ψ, thereby tending to cancel the effect due to the increase in τ.

A most remarkable feature of Figure 21 is the existence of a unique relationship between the exponent γ and ψ for all the flare events. This implies that either (a) the source spectrum is the same for all flare events or (b) no matter what the initial source spectrum is, the spectrum at late times during decay is completely determined by the convective and diffusive properties of the interplanetary medium; i.e., the spectral property of the solar flux at any point is only a function of its distance from the centroid of the population.

The fact that the spectral exponent is a function of the angular distance from the parent flare is clearly related to the process whereby the cosmic radiation propagates to field lines far distant from the flare. Thus Figure 21 indicates that the propagation is more effective at higher energies, which is in qualitative agreement with any concept of 'near Sun' diffusion. Given a more thorough understanding of the functional dependence of cosmic ray density upon ψ, the variation of γ will permit a quantitative test of specific near-Sun diffusion models.

The data available at present are insufficient to resolve the quantitative details of the various functional dependencies upon ψ. A greater body of data concerning the concurrent gradients, anisotropies and time constants in the energy range 1–50 MeV will be exceedingly fruitful in this regard. In our opinion, such data will lead, for the first time, to sufficient quantitative knowledge of the particle removal phenomena to

permit meaningful tests of the contemporary theories regarding the escape of solar cosmic rays from the solar system.

At the time of writing (September 1970), the four Pioneer spacecraft discussed herein are still operational and they are still producing data of similar quality to those reported herein. With the co-operation of the Sun, therefore, we hope to resolve many of the questions defined in this paper in the near future.

8. Conclusions

We conclude by summarizing the properties of the cosmic radiation at times $T \gtrsim 1$ day after a solar flare injection.

1. ANISOTROPY

1.1. At $T \lesssim 4$ days, the anisotropy at $E \simeq 10$ MeV tends to be directed radially away from the Sun.

1.2. At $T \gtrsim 4$ days, the anisotropy at $\simeq 10$ MeV is directed from a direction $\simeq 45°$ E of the satellite-Sun line.

1.3. We suggest that the anisotropy is parallel to the vector $\mathbf{E} \times \mathbf{B}$ at very late times ($T \gtrsim 4$ days).

2. CONVECTIVE REMOVAL PROCESSES

2.1. Properties 1.1 and 1.2 imply the dominance of convection as compared to diffusion in the escape of solar cosmic rays from the solar system at late times ($T \gtrsim 1$ day).

2.2. A positive radial cosmic ray density gradient, $\partial U/\partial s$, exists at very late times ($T \gtrsim 4$ days) near orbit of Earth. This drives a diffusive current along the interplanetary magnetic field lines towards the Sun.

2.3. The effective convective removal velocity will be $< V_p$ at very late times. It approximates 0.5 V_p at such times as the anisotropy is from 45° E of the Sun, at orbit of Earth.

2.4. An anisotropy normal to **B** implies an equilibrium between the convective current $V_p U$, and the diffusive current $K\, \mathrm{d}U/\mathrm{d}s$ along the interplanetary field lines, where V_p is the component of the solar wind velocity parallel to the interplanetary magnetic field.

3. SPATIAL GRADIENTS

3.1. As noted in 2.2, the properties of the cosmic ray anisotropy imply a positive radial gradient of cosmic ray density at very late times ($T \gtrsim 4$ days).

3.2. Direct measurements indicate the persistence of strong gradients in heliocentric longitude at very late times ($T \gtrsim 4$ days). e-folding angles of $|\eta_0| \simeq 30°$ have been observed.

3.3. At very late times ($T \gtrsim 4$ days) the relative gradient $(1/U\, \mathrm{d}U/\mathrm{d}\theta)$, in heliocentric longitude is invariant with respect to time.

4. Temporal decay

4.1. The observed temporal variation of the cosmic ray flux is due to two major effects (a) convective removal of the cosmic radiation (b) the 'co-rotation' of the cosmic ray population, (see Equation (2)).

4.2. The observed time rate of change of cosmic ray flux is critically dependent upon the local value of the gradient in heliocentric longitude (for $E \lesssim 10$ MeV). When the observer is to the west of the centroid of the cosmic ray population, the gradient has been observed to result in the almost complete cancellation of the temporal decay which is due to the expulsion of the cosmic radiation by the solar wind. When the observer is to the East of the population centroid, the effect is to hasten the decay by a factor of $\simeq 2$.

4.3. The properties of the cosmic ray spectra indicate that the influence of the longitude gradient upon the observed temporal decay increases towards lower energies. For example, for the flare event of 1969, March 29, the gradient term at about 5 MeV exceeds the convective removal term in Equation (5). In this case, an observer on the western side of a cosmic ray population sees a flux that increases with time.

4.4. The convective component of the decay time constant, τ, is expressible in terms of the characteristics of the anisotropy (Equation (9)).

4.5. The convective time constant, τ, increases by a factor of ~ 2 between the epoch when the anisotropy is directed from the Sun, to the epoch at which it is directed from 45° E.

4.6. At late times, when the anisotropy is directed from the Sun, $(1 \lesssim T \lesssim 4)$, the convective time constant varies as the reciprocal of the solar wind velocity. At very late times, $(T \gtrsim 4$ days) it is essentially independent of V_p.

4.7. The observed time constant T is a function of the position of the observer relative to the centroid of the cosmic ray population.

5. Cosmic ray spectrum

5.1. At late times, $(T \gtrsim 2$ days), the spectral exponent near 10 MeV is dependent on the longitude of the observer relative to the centroid of the cosmic ray population injected by the flare. This effect results in a variation in spectral exponent over the range $2.0 < \gamma < 4.5$.

5.2. At a given point in the frame of reference of the cosmic ray population, the spectral exponent is invariant with time.

Acknowledgements

The authors wish to express their indebtedness to Mr. W. C. Bartley and Mr. J. M. Younse for their active role in the development of the Pioneer instruments. Assistance of many kinds was provided by the Pioneer Project Manager, Mr. C. F. Hall and his staff. The authors are grateful to Messrs. E. H. Lax and D. D. Mosier and Mrs. M. D. Luna for their assistance in the analysis of the data.

This research was supported by funds from the National Aeronautics and Space Administration under Contracts NSR-44-004-043, NAS2-3332, NAS2-4674, NGR-44-004-108, NAS2-3945, and funds from 'Excellence in Education Foundation'. One of us (U.R.R.) wishes to acknowledge the travel support provided by the grant NAS-1492 from the National Academy of Sciences, U.S.A.

References

Ahluwalia, H. S. and Dessler, A. J.: 1962, *Planetary Space Sci.* **9**, 195.
Allum, F. R., Rao, U. R., McCracken, K. G., Palmeira, R. A. R., and Harries, J. R.: 1970 (under publication).
Bartley, W. C., McCracken, K. G., and Rao, U. R.: 1967, *Rev. Sci. Instr.* **38**, 266.
Bukata, R. P., Keath, E. P., Younse, J. M., Bartley, W. C., McCracken, K. G., and Rao, U. R.: 1970, *IEEE, Transactions in Nuclear Science.*
Bukata, R. P., Rao, U. R., McCracken, K. G., and Keath, E. P.: 1971 (under publication).
Forman, M. A.: 1970, *J. Geophys. Res.* **75**, 3147.
McCracken, K. G., Rao, U. R., and Bukata, R. P.: 1967, *J. Geophys. Res.* **73**, 4159.
McCracken, K. G., Rao, U. R., and Ness, N. F.: 1968, *J. Geophys. Res.* **73**, 4159.
McCracken, K. G. and Rao, U. R.: 1970, *Space Sci. Rev.*
Parker, E. N.: 1965, *Planetary Space Sci.* **13**, 9.
Rao, U. R., McCracken, K. G., Allum, F. R., Palmeira, R. A. R., Bartley, W. C., and Palmer, I.: 1970 (under publication).
Smerd, S. F.: 1970, *Proc. Astron. Soc. Australia*, No. 7 (preprint).